NATIONAL UNIVERSITY OF SCIENCE AND
TECHNOLOGY POLITEHNICA BUCHAREST
DOCTORAL SCHOOL OF ENERGY ENGINEERING
FUNDAMENTAL FIELD OF DOCTORAL STUDIES:
ENGINEERING SCIENCES
DOCTORAL FIELD: ENERGY ENGINEERING

DOCTORAL THESIS
ABSTRACT

MODERN DISTRIBUTION SYSTEMS

Scientific Supervisor :
Prof. emerit dr. ing. Nicolae GOLOVANOV

PhD Student :
ing. Valentin DOBRE

București, 2025

1. Distribution Networks in the Energy Transition

Distribution networks represent the infrastructure through which more than 95% of end users are supplied with electricity. They are, therefore, the most exposed component to the transformations brought by the integration of distributed generation and the electrification of transport. Substations, medium- and low-voltage lines, as well as protection and automation equipment, are becoming critical elements in ensuring continuity, quality, and supply reliability.

1.1 Identified Issues and Research Directions

The evolution of distribution systems entails the emergence of challenges that require innovative solutions:

- **Reverse power flow –** generated by active users and distributed generation sources (DGS), it can lead to equipment overloading, improper operation of protection systems, and reduced transformer lifespan;
- **Loss of load predictability –** with the emergence of electric vehicles and prosumers, the load profile becomes significantly more volatile;
- **Structural limitations of existing networks –** many of them were designed for consumption conditions that differ substantially from current ones;
- **Integration of BESS (Battery Energy Storage Systems) –** which can balance production and consumption variations but also introduces challenges in terms of sizing, control, and costs.

1.2 Objectives of the Doctoral Thesis

The central objective of this thesis is the analysis and modeling of the impact generated by the integration of distributed renewable sources and reverse power flow on electrical distribution networks, with a particular focus on the technical and economic solutions required to enhance efficiency and reliability.

2. STRUCTURE OF A DISTRIBUTION SYSTEM

2.1 Reconfiguration. Use of Automated Reclosers in Medium-Voltage Networks

The implementation of automated circuit breakers (reclosers) along medium-voltage (MV) lines represents an essential measure for enhancing network reliability and self-healing capability. These devices can be integrated within the following operational contexts:

- on already automated medium-voltage lines, where a high number of switchings or trippings are expected due to transient or permanent faults;
- in automated networks equipped with Centralized Functionalities (CF), when the maximum allowable number of sectionalizing switches in a serial topological configuration has been exceeded;
- to ensure automatic reclosing functionality, regardless of the neutral grounding mode (isolated, resistance-grounded, or via Petersen coil), and independently of the existence of an extended automation system.

To ensure protection selectivity, it is often necessary to introduce a time delay within the primary substation protection scheme. This delay allows the MV circuit breaker in the

intermediate field to clear the fault without causing a cascading trip of the entire feeder. In such cases, it is essential to verify whether the network elements located between the recloser and the transformer substation (conductor, equipment, insulation) can withstand the additional thermal stress generated by a sustained three-phase short-circuit current.

2.2 Benefits of Implementing Remote Control and Automation in Medium-Voltage Networks

The main benefits can be grouped into the following categories:

- **Increased reliability and operational efficiency**
  - reduction of the number of consumers affected by interruptions lasting more than 3 minutes;
  - shortening of maneuver execution time during network reconfiguration;
  - limitation of the network portion requiring manual intervention for fault isolation;
  - reduction of the workload for control center operators through automatic fault localization and section selection.
- **Support for the energy transition and network digitalization**
  - dynamic reconfiguration of the network based on the optimal operating topology;
  - redistribution of load flows to minimize losses;
  - rapid adaptation to variable operating conditions through the use of sensors, bidirectional communications, and advanced SCADA systems.
- **Improvement of customer satisfaction**

By reducing the duration and frequency of interruptions, remote control and automation directly contribute to increasing customer satisfaction. The reduced outage time translates into improved supply continuity for residential, commercial, and industrial consumers, mitigating the economic impact of unplanned outages.

- **Enhanced network resilience**
  - maintaining supply for a significant portion of consumers;
  - minimizing the number of disconnected sections during the initial stages of fault isolation;
  - reducing the spread of the area affected by the disturbance event.
- **Improved safety and reduced environmental impact**
  - enhancement of safety indicators for operational personnel;
  - reduction in the incidence of occupational accidents in medium-voltage networks.

2.2.1 Improving Network Reliability through Remote Control – Impact on SAIDI and SAIFI Indicators

For illustration purposes, a simplified radial configuration is considered (as shown in Fig. 2.10), in which the medium-voltage (MV) line supplies a total of $C_{total} = 100$ users, uniformly distributed along its route. It is assumed that the probability of fault occurrence is uniform over the entire line length, and that the circuit breaker located in the HV/MV substation is remotely operated.

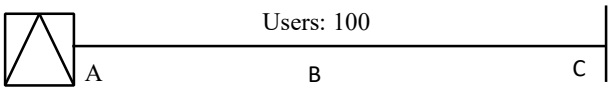


Fig. 2.10 – Simplified diagram of the radial line

Considering initially the line operating without remote control and then introducing a remotely controlled point (for example, a recloser) at a strategic node of the network, the relative value $SAIDI_{RCP}$ results from the following relation:

$$SAIDI_{RCP\%} = \frac{SAIDI_{RCP1}}{SAIDI_{RCP}} \cdot 100 = \frac{\frac{\sum C_{int} \cdot Durata}{C_{total}}}{\frac{\sum C_{int0} \cdot Durata}{C_{total}}} \cdot 100, \qquad (2.2)$$

where:

$SAIDI_{RCP1}$ represents the value of the *SAIDI i*ndicator in the case of a control node,

$SAIDI_{RCP0}$ – represents the value of the *SAIDI i*ndicator in the case of a line without a control node,

C_{int} – represents the number of users associated with the corresponding interruption durations,

C_{int0} – represents the number of users associated with the corresponding interruption durations, in the absence of the control node

2.2.2 Medium-Voltage Network with Remote Control and the Possibility of Alternative Supply from Other Sources

When the network architecture allows the line to be re-energized from an alternative endpoint, after identifying and isolating the faulty section, the final stage of the intervention consists of restoring power supply to part of the consumers through remote commands..

The maximum number of re-energized customers ($C_{\,re-energ\,.\,MAX}$) depends on the line's resupply capability ($Re-Re-negn_{\,\%}$).

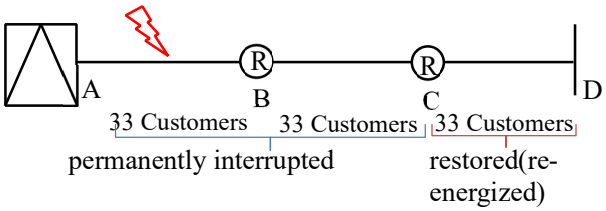


Fig.2.19 Feeder re-energized with two remotely controlled devices (Fault in section AB)

	Localizarea defecțiunii AB		
	Număr	Durată	
C int–perm	66	D	Secțiunea AC
C recuperați	0		-
C realimentați.	33	TLC_{time}	Secțiunea CD

$$C_{\,re-energ\,.\,MAX} = Re-energ\,._{\%} \cdot C_{\,tot} \qquad (2.16)$$

It is assumed that a permanent fault occurs in section **AB**. The evolution of the event can be divided into three operational phases (Fig. 2.19):

a. **Initial tripping.** The circuit breaker in the source substation detects the fault and opens, leading to the interruption of all consumers along the line.
b. **Fault localization and isolation**. Through remote-control operations, the faulty section is located; the substation circuit breaker and the recloser at node B are opened. Customers located between A and B will be permanently interrupted.
c. **Partial restoration.** Although all consumers downstream of point B (66%) could be re-energized from the opposite end, the available resupply capacity (50%) is insufficient for the entire load. Therefore, the operator opens node C (segmenting the downstream line) and closes D, thereby restoring supply only to customers located between C and D, representing 33% of the total. Customers between B and C remain permanently interrupted, while those between C and D are re-energized.

$$SAIDI_{ABfault} = D \cdot \left(\frac{66 + 33 \cdot \frac{TLC_{time}}{D}}{100} \right) \cdot (1 + 0{,}05) = 0{,}695 \cdot D$$

If the fault is located in section **BC** (see Fig. 2.20):

1. The customers in section **AB** will be restored.
2. The customers in section **BC** will be permanently interrupted.
3. The customers in section **CD** will be re-energized.

$$SAIDI_{BCfault} = D \cdot \left(\frac{33 + 66 \cdot \frac{TLC_{time}}{D}}{100} \right) \cdot (1 + 0{,}05) = 0{,}352 \cdot D$$

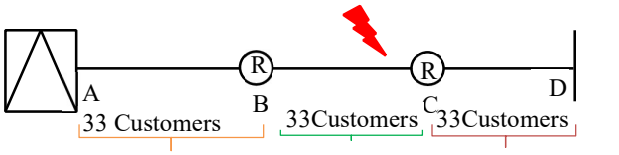


Fig.2.20 Feeder re-energized with two remotely controlled devices (Fault in section BC)

	Localizarea defecțiunii BC		
	Număr	Durată	
C int–perm	33	D	Secțiunea BC
C recuperați	33	*TLC time*	Secțiunea AB
*C re–*alimentați.	33	*TLC time*	Secțiunea CD

If the fault is located in section CD (see Fig. 2.21):

1. The customers in section AB will be restored;
2. The customers in section BC will be restored;
3. The customers in section CD will be permanently interrupted

$$.SAIDI_{CD\ defect} = D \cdot \left(\frac{33+66\cdot\frac{TLC_{timp}}{D}}{100}\right) \cdot (1+0{,}05) = 0{,}352 \cdot D$$

To obtain $SAIDI_{TLC\,\%}$ it is necessary to compare the $SAIDI$ value obtained in these final simulations with the value obtained without remote control.

$$SAIDI_{TLC\%} = 100 \cdot \frac{SAIDI_{2TLC(re-energ)(defect\ AB+defec\ \ BC+defec\ \ CD)}}{SAIDI_{0-TLC(defect\ AB+defec\ \ BC)}}$$
$$= 100 \cdot \frac{0{,}695D + 0{,}352D + 0{,}352D}{D+D+D} = 46{,}6\% \qquad (2.17)$$

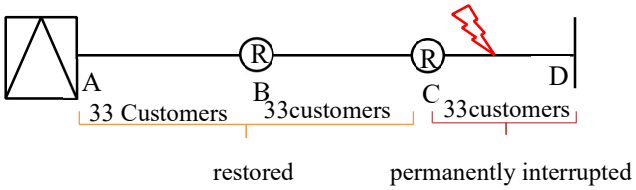


Fig.2.21 Feeder re-energized with two remotely controlled devices (Fault in section CD)

	CD cu locația defecțiunii		
	Număr	Durată	
C int–perm	33	D	Secțiunea CD
C recuperați	66	TLC_{time}	Secțiunea AC
C re–energ.	0	-	-

The SAIDI (*System Average Interruption Duration Index*) values show significant improvements as the number of Remote Control Points – RCP installed along the medium-voltage network increases. These devices contribute to the segmentation of the network, reducing the average duration of interruptions by enabling faster fault identification and isolation. However, the marginal benefit of each additional remotely controlled device decreases progressively.

This phenomenon is reflected in the shape of the SAIDI evolution curve, which tends toward an asymptote. Thus, as the number of sections defined by remote-control devices increases, the additional efficiency gained from adding a new device becomes progressively smaller.

In parallel, another essential factor influencing SAIDI is the resupply level of the network, expressed as the percentage of total load capacity that can be restored from alternative sources. The higher this level, the more consumers can be re-energized after isolating a fault, leading to a further reduction in the average duration of interruptions.

Figure 2.23 presents the $SAIDI_{RCP\%}$ trend curves as a function of the number of remotely controlled devices and the level of resupply.

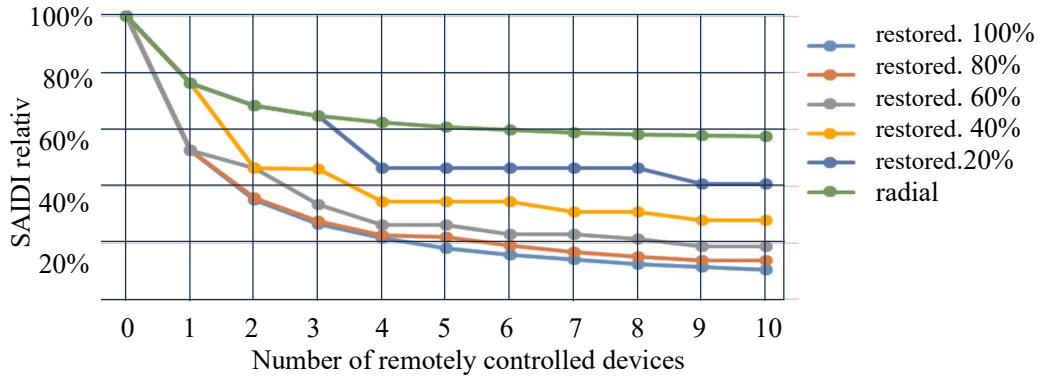


Fig.2.23 Trend curves of SAIDIRCP%

The curves presented in Figure 2.23 highlight that the marginal benefit brought by each new remote-control point is not constant but may exhibit local discontinuities.

This non-uniformity reflects the limitations of the adopted model, which assumes:

- a uniform distribution of consumers along the line;
- a resupply capacity expressed as a constant percentage;
- the absence of constraints related to current or voltage limits during resupply.

2.4 Smart Grids and Modern Challenges

Modern distribution systems must integrate:

- distributed renewable energy sources (DER),
- electric vehicle (EV) charging stations,
- advanced metering infrastructure (AMI),
- automation systems (FLISR, SCADA, DMS).

Smart Grids involve the bidirectional flow of both energy and information, requiring a new framework for design and operation [2.11].

The increasing penetration of decentralized generation resources in medium- and low-voltage networks — such as photovoltaic plants, combined heat and power (CHP) microturbines, small wind turbines, and, in the future, fuel cells — fundamentally changes the traditional operating principle of electric networks [2.13], [2.14]. A particularly promising aspect of the proliferation of these distributed sources is the possibility for certain portions of the network, endowed with sufficient generation resources, to operate independently from the main grid in a deliberate, controlled, and secure manner. These structures are known as microgrids, and research and demonstration projects carried out over recent decades have shown their significant potential for efficient integration into distribution systems [2.15], [2.16].

The main advantage of proximity between generation sources and loads lies in the reduction of transmission and distribution losses, as well as in the mitigation of network congestion phenomena [2.17]. Moreover, microgrids enhance the reliability of power supply to end users, since local generation resources, controllable loads, and energy storage systems can operate in islanded mode during severe disturbances in the main grid [2.18]. Other major benefits include lower overall energy consumption, reduced environmental impact, and improved supply reliability levels [2.19].

2.4.1 Components of Microgrids

A microgrid consists of four essential elements [2.15], [2.18]:

a) **Local generation** – distributed sources, typically renewable or cogeneration-based;
b) **Energy Management System (EMS)** – coordinates generation, storage, and consumption;
c) **Load controller** – regulates the operation of controllable consumers and optimizes the load profile;
d) **Interface with the main grid** – ensures synchronization, protection, and bidirectional energy exchange.

3 LOSSES IN THE CURRENT SYSTEM AND IMPROVEMENT PROPOSALS

3.1 Loss Reduction Strategies

Actions aimed at reducing total energy losses (CPT) focus on both technical and commercial losses.

Technical Loss Reduction:

- Replacement of MV/LV transformers with a loading rate above 80% and an operating age over 30 years with modern units featuring reduced losses and fine voltage adjustment capability (from ±5% to ±2 × 2.5%) [3.12];
- Replacement of underloaded transformers with units of appropriate rated power;
- Construction of new medium-voltage injection points (distribution substations) to reduce LV network length [3.13];
- Load balancing across phases;
- Increasing conductor cross-sections;
- Load flow redistribution by transferring demand to less-loaded network elements;
- Optimization of operating schemes at all voltage levels [3.14];
- Installation of new substations and dedicated lines to limit LV network lengths exceeding 0.5 km;
- Transition to higher voltage levels (e.g., 10 kV → 20 kV; 0.38 kV → 0.4 kV) [3.15];
- Network reconstruction in correlation with increasing consumption density;
- Modernization of metering systems through the installation of smart meters [3.16];
- Implementation of ADMS (Advanced Distribution Management Systems) for operating regime optimization;
- Installation of reactive power compensation equipment.

Commercial Loss Reduction:

- Installation of Metering and Protection Units (MPUs);
- Securing distribution boxes and service cabinets;
- Relocation of meters to operator-accessible areas [3.17];
- Equipping operational teams with high-precision measuring instruments;
- Implementation and modernization of IT systems to reduce reading and billing errors;

- Targeted inspections based on consumption analysis and data provided by smart meters [3.18];
- Cooperation with authorities to detect illegal connections in high-risk areas.

Numerical Example – Reduction of Joule Losses after Modernization

A 10 km power line transporting 5 MW is considered [3.16]:

- Initial situation:
  – Voltage: 10 kV
  – Resistance: 0.2 Ω/km
  – Joule losses: 3.33% of transmitted power
- After modernization:
  – Voltage: 20 kV
  – Resistance: 0.1 Ω/km (increased conductor cross-section)
  – Joule losses: 0.42% of transmitted power

Conclusion: Following the line modernization, Joule effect losses are reduced by 2.92 percentage points, corresponding to a relative reduction of approximately 87.5%.

3.2 Network Component Replacement – Transformer Modernization and Upgrading

Improving the energy efficiency of distribution networks requires planned interventions on equipment with a major impact on losses, particularly power transformers located in substations and distribution stations. Within this study, two types of measures were analyzed:

a) Replacement of existing transformers with "low-loss" units of the same rated power;
b) Upgrading of transformer substations by replacing existing transformers with higher-rated units, optimally dimensioned for the actual load conditions.

3.2.1 Replacement of Existing Transformers with Low-Loss Units

The evaluation of annual losses was carried out according to the relationships provided in the specialized literature and international standards [3.22], [3.23]:

$$Etot = Pfe * T + Pcu * \tau, \quad (3.1)$$

where:

- T – annual operating time of the transformer [h/year],
- τ – equivalent time at rated current [h/year], calculated from the load profile,
- $P_{(fe)}$ – no-load (core) losses [W],
- $P_{(cu)}$ – copper losses at rated current [W].

The comparative analysis for **250 kVA**, **400 kVA**, and **630 kVA** transformers revealed significant reductions in annual losses when transitioning from standard equipment to **low-loss units**, while maintaining the same rated power (Table 3.1).

Table3.4 – Loss Reduction through Replacement with "Low-Loss" Transformers

Rated Power (kVA)	Annual Losses – Standard (kWh/an)	Annual Losses – Low-Loss (kWh/an)	Energy Benefit (MWh/an)
250	7.923,95	5.033,15	2,89
400	11.551,01	7.171,01	4,38
630	16.198,29	10.066,29	6,13

The results indicate a percentage reduction in losses between 27% and 38%, depending on the rated power, with the annual cumulative benefit being significant in areas with high consumption density (Fig. 3.2).

The energy benefits are direct and quantifiable, with a cumulative effect over the equipment's lifetime (20–30 years), which justifies the investment even in cases of higher initial costs [3.24], [3.25].

3.2.2 Transformer Substation Upgrade

Table 3.7 – Loss Reduction through Transformer Substation Upgrading

Configuration	Annual Losses (kWh/an)	Energy Benefit (MWh/an)
250 → 400 kVA	7.171,01	0,75
400 → 630 kVA	10.066,29	1,48

Deși beneficiile absolute sunt mai reduse decât în cazul înlocuirii echipamentelor la aceeași putere, amplificarea postului poate aduce avantaje suplimentare în ceea ce privește capacitatea de preluare a sarcinii, reducerea pierderilor Joule în rețelele secundare și îmbunătățirea calității tensiunii la consumator [3.26].

Although the absolute benefits are lower than in the case of replacing equipment with the same rated power, upgrading the transformer substation can provide additional advantages in terms of load-handling capacity, reduction of Joule losses in secondary networks, and improvement of voltage quality at the consumer end [3.26].

Technical and Economic Considerations

- Energy impact: Reducing energy losses through transformer modernization has a direct effect on the overall efficiency of the network and on operating costs [3.26].
- Economic impact: The resulting energy savings can be quantified and converted into annual financial savings using the average electricity tariff applied to network losses (CPT).
- Lifetime and amortization: The benefits accumulate over the equipment's service life, justifying the investment even in cases of higher initial costs.
- Integration into network strategy: The measures must be correlated with other network optimization actions (phase balancing, reactive power compensation, conductor cross-section increase) to maximize the overall effect [3.27], [3.28].

3.2.3 Analysis of Losses in Medium-Voltage Power Lines

Within medium-voltage (MV) distribution networks, energy losses are directly influenced by the construction characteristics of conductors, the type of installation (overhead line – OHL or underground cable – UGC), as well as by operating parameters such as load current, power factor, and conductor resistance.

This assessment does not include indirect benefits, such as reduced maintenance costs, increased supply continuity, or the mitigation of penalties associated with service interruptions.

Table 3.10 – Economic Indicators

Configuration	Annual Losses (MWh)	Loss Cost (lei/an)	Annual Energy Benefit (MWh)	Annual Savings (lei)
LEA 3×35 mm² – 1 km	11,92	5.364	–	–
LEA 3×50 mm² – 1 km	8,48	3.816	3,44	1.548
LEA 3×70 mm² – 1 km	6,22	2.799	5,70	2.565
LES 3×1×185 mm² – 1 km	0,85	383	11,07	4.981
LES 3×150 mm² – 1 km	3,32	1.494	8,60	3.870
Conversion OHL → UGC (Example)				
LEA 3×70 mm² – 27 km	222,25	100.012	–	–
LES 3×1×185 mm² – 33 km	86,11	38.750	136,14	61.263

Replacement of Overhead Power Lines (OHL) with Underground Cables (UGC) of Increased Cross-Section

Modernizing the electricity distribution infrastructure by replacing overhead lines (OHL) with underground cables (UGC), implemented through the installation of cables with enlarged cross-sections, represents an increasingly adopted solution in the context of rapid urbanization and the need to enhance the reliability and safety of electrical networks. This intervention is justified both from technical and economic perspectives, leading to improved network performance parameters and a reduced visual impact on the urban environment.

Advantages

- **Improved urban aesthetics**. The removal of poles and overhead conductors significantly enhances the visual appearance of urban areas, increasing their attractiveness for developers and residents.
- **Reduced environmental impact**. Eliminating above-ground structures minimizes the impact on the landscape and natural habitats, especially in ecologically sensitive areas.
- **Increased reliability**. Underground cables are less vulnerable to extreme weather phenomena (storms, strong winds, freezing), which significantly reduces the risk of faults and power supply interruptions [3.31].
- **Enhanced public safety**. The elimination of risks associated with accidental contact or pole collapse reduces the likelihood of accidents involving both the public and maintenance personnel.
- **Elimination of interferences**. In dense urban environments, overhead lines can interfere with buildings, transport infrastructure, or other utility networks. Replacing them with UGC avoids these spatial conflicts.

Economic Considerations

- **High initial costs**. The upfront investment in UGC is considerably higher than in OHL, due to the costs of materials (insulated cables, protective elements) and infrastructure works (excavation, installation, and road restoration).

- **Reduced maintenance costs**. UGCs involve lower maintenance expenses thanks to protection from external factors. However, in case of faults, locating and repairing them is more complex and costly than for overhead lines.
- **Lower operational costs**. The absence of above-ground components (poles, insulators, brackets) reduces costs associated with periodic inspections and structural repairs.
- **Indirect costs**. Undergrounding works can cause disruptions to traffic and local economic activity, requiring compensatory measures and good logistical planning.
- **Extended service life.** UGCs generally have a longer lifespan compared to OHLs due to protection against environmental wear, which reduces replacement investment frequency.
- **Higher energy efficiency**. By using conductors with larger cross-sections and reduced linear resistance, energy losses are minimized, contributing to the economic optimization of the network.
- **Increase in real estate value**. The removal of overhead infrastructure can lead to an appreciation in land and building value near the route, stimulating urban development.

Technical Considerations

- **Increased transmission capacity.** UGCs with enlarged conductor cross-sections allow greater power transfer, adapting the network to the rising consumption demands of urban areas.
- **Improved reliability**. Protection against weather, vandalism, and other external factors increases network availability and reduces the average duration of outages [3.32].
- **Reduced technical losses.** Selecting conductors with appropriate cross-sections decreases Joule losses, thereby improving the network's energy efficiency.
- **Enhanced operational safety.** Eliminating risks of direct contact with conductors or pole collapse provides significant benefits for network safety [3.32], [3.33].
- **Reduced impact on the built environment**. UGCs enable better integration into urban areas without affecting existing infrastructure elements or public space aesthetics.

3.3 Case Study: Calculation of Losses on a Medium-Voltage Line

The analyzed line has a nominal voltage of 20 kV and the radial structure shown in Figure 3.3. In calculating the losses on the cable line compared to those on the overhead line, the following assumptions were made:

- dielectric (shunt) losses of the lines were neglected;
- the short-circuit power at the supply point of the line was assumed to be determined solely by the HV/MV supply transformer;
- losses in the MV/LV transformers were not calculated, assuming they have the same values in both line-equipment scenarios;
- line loading was considered symmetrical and the currents sinusoidal;
- the calculation program used to determine the losses on the 20 kV radial line was developed based on the loss time method, using the relation given in [3.2].

$$\tau = T_f \cdot [p \cdot k_u + (1 - p) \cdot k_u^2], \tag{3.2}$$

Where:

T_f – operating time [h];

p = 0,2 (calculation factor);

k_u –load factor (for the load curves in the analyzed scheme, an estimated value of *ku= 0,3456* was used. From relation (3.2), the result is τ *=1442,93 hours*.

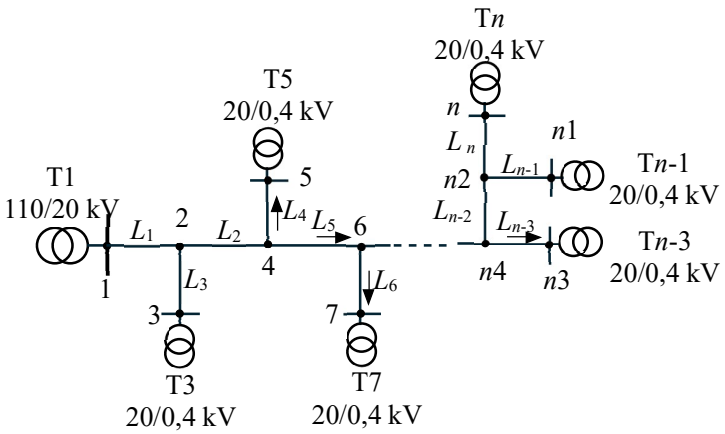


Fig. 3.3 Structure of the analyzed radial network..

The estimation of active ΔWa and reactive ΔWr losses was carried out based on the maximum hourly values of active energy Wa,max and reactive energy Wr,max for each line segment *k* of the network.

$$\Delta W_a = \frac{\tau}{U_N^2} \cdot \sum_{k=1}^{n_L} R_k \cdot (W_{ka,max}^2 + W_{kr,max}^2), \qquad (3.3)$$

where n_L is the number of line sections considered.

The voltages at the nodes of the analyzed network can be determined based on the current values calculated from the hourly energy measurements provided by the energy meters installed at the network nodes and the corresponding line section impedances.

The calculation program used to determine energy losses in medium-voltage electrical networks includes the following components:

Table 3.11 – Input Data

Mărime	Valoare
T_f[h]	8760,00
T_{rsm} [h]	1914,19
τ [h]	1725,01
I_{max} [A]	95,60
S_{max} [kVA]	3307,76
W_a(MWh)	2395,00
W(MVARh)	2876,82
U(kV)	20
S_{inst} [kVA]	5500
S_{max}/S_{inst} [-]	0,601
PF[-]	0,92
tan φ	0,402716

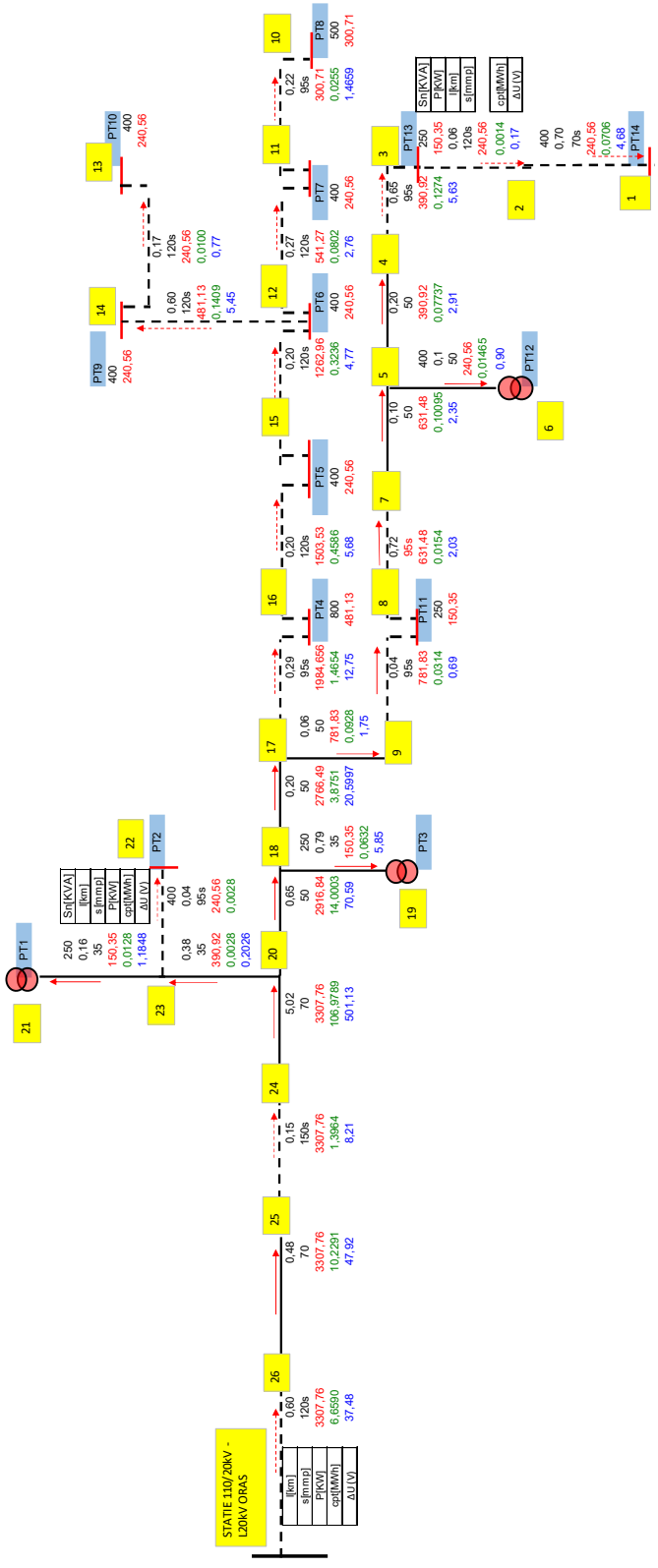


Fig. 3.4 Calculation Results

Tabelul 3.12 Calculation Data

Section	LEA/ LES	*s* [mmp]	Length [km]	*P* [kW]	*I* [A]	r_0 [Ω/km]	x_0 [Ω/km]	Annual losses [MWh]	Δ*U* [V]	Δ*U* [%]
1-2	LES	70s	0,70	240,56	7,55	0,409	0,364	0,0706	4,68	0,023
2-3	LES	120s	0,06	150,35	4,72	0,238	0,347	0,0014	0,17	0,001
3-4	LES	95s	0,65	390,92	12,27	0,301	0,353	0,1274	5,63	0,028
4-5	LEA	50	0,20	390,92	12,27	0,594	0,374	0,0774	2,91	0,015
5-6	LEA	50	0,10	240,56	7,55	0,594	0,374	0,0147	0,90	0,004
5-7	LEA	50	0,10	631,48	19,81	0,594	0,374	0,1010	2,35	0,012
7-8	LES	95s	0,70	130,85	4,11	0,301	0,353	0,0154	2,03	0,010
8-9	LES	95s	0,04	781,83	24,53	0,301	0,353	0,0314	0,69	0,003
10-11	LES	95s	0,22	300,71	9,44	0,301	0,353	0,0255	1,47	0,007
11-12	LES	120s	0,27	541,27	16,98	0,238	0,347	0,0802	2,76	0,014
13-14	LES	120s	0,17	240,56	7,55	0,238	0,347	0,0100	0,77	0,004
14-12	LES	120s	0,60	481,13	15,10	0,238	0,347	0,1409	5,45	0,027
12-15	LES	120s	0,20	1.262,96	39,63	0,238	0,347	0,3236	4,77	0,024
15-16	LES	120s	0,20	1.503,53	47,18	0,238	0,347	0,4586	5,68	0,028
16-17	LES	95s	0,29	1.984,66	62,27	0,301	0,353	1,4654	12,75	0,064
9-17	LEA	50	0,06	781,83	24,53	0,594	0,374	0,0928	1,75	0,009
17-18	LEA	50	0,20	2.766,49	86,81	0,594	0,374	3,8751	20,60	0,103
18-19	LEA	35	0,79	150,35	4,72	0,830	0,385	0,0632	5,85	0,029
18-20	LEA	50	0,65	2.916,84	91,52	0,594	0,374	14,0003	70,59	0,353
21-23	LEA	35	0,16	150,35	4,72	0,830	0,385	0,0128	1,18	0,006
22-23	LES	95s	0,04	240,56	7,55	0,301	0,353	0,0028	0,20	0,001
20-23	LEA	35	0,38	390,92	12,27	0,830	0,385	0,2054	7,32	0,037
20-24	LEA	70	5,02	3.307,76	103,79	0,457	0,364	106,9789	501,13	2,506
24-25	LES	150s	0,15	3.307,76	103,79	0,194	0,340	1,3964	8,21	0,041
25-26	LEA	70	0,48	3.307,76	103,79	0,457	0,364	10,2291	47,92	0,240
26-STATIE	LES	120s	0,60	3.307,76	103,79	0,238	0,347	6,6590	37,48	0,187
Total losses (MWh)					**146,46**					

When converting the overhead lines to underground cables (**Fig. 3.5**), the calculation data obtained are presented in **Table 3.13**.

Fig. 3.2 Rezultate de calcul

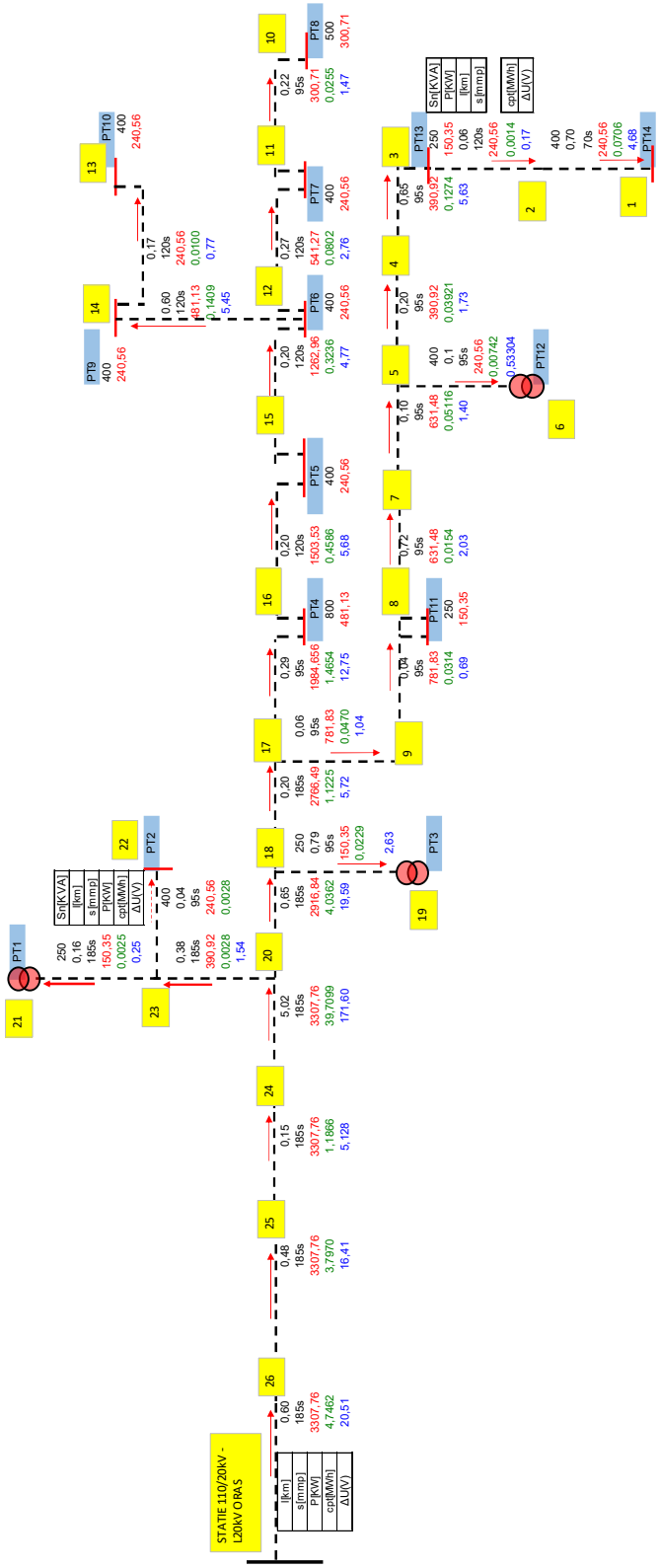


Fig. 3.5Calculation Results for the Overhead-to-Underground Line Conversion

Table 3.13 – Calculation Results for the Conversion of Overhead Lines to Underground Cables

Section	LEA/ LES	*s* [mmp]	Length [km]	*P* [kW]	*I* [A]	r_0 [Ω/km]	x_0 [Ω/km]	Annual losses [MWh]	Δ*U* [V]
1-2	70s	0,70	240,56	7,55	0,409	0,364	0,0706	4,678	0,0234
2-3	120s	0,06	150,35	4,72	0,238	0,347	0,0014	0,170	0,0009
3-4	95s	0,65	390,92	12,27	0,301	0,353	0,1274	5,630	0,0282
4-5	95s	0,20	390,92	12,27	0,301	0,353	0,0392	1,732	0,0087
5-6	95s	0,10	240,56	7,55	0,301	0,353	0,0074	0,533	0,0027
5-7	95s	0,10	631,48	19,81	0,301	0,353	0,0512	1,399	0,0070
7-8	95s	0,70	130,85	4,11	0,301	0,353	0,0154	2,030	0,0101
8-9	95s	0,04	781,83	24,53	0,301	0,353	0,0314	0,693	0,0035
10-11	95s	0,22	300,71	9,44	0,301	0,353	0,0255	1,466	0,0073
11-12	120s	0,27	541,27	16,98	0,238	0,347	0,0802	2,760	0,0138
13-14	120s	0,17	240,56	7,55	0,238	0,347	0,0100	0,772	0,0039
14-12	120s	0,60	481,13	15,10	0,238	0,347	0,1409	5,452	0,0273
12-15	120s	0,20	1.262,96	39,63	0,238	0,347	0,3236	4,771	0,0239
15-16	120s	0,20	1.503,53	47,18	0,238	0,347	0,4586	5,679	0,0284
16-17	95s	0,29	1.984,66	62,27	0,301	0,353	1,4654	12,753	0,0638
9-17	95s	0,06	781,83	24,53	0,301	0,353	0,0470	1,039	0,0052
17-18	185s	0,20	2.766,49	86,81	0,164	0,106	1,1225	5,718	0,0286
18-19	95s	0,79	150,35	4,72	0,301	0,353	0,0229	2,632	0,0132
18-20	185s	0,65	2.916,84	91,52	0,164	0,106	4,0362	19,593	0,0980
21-23	185s	0,16	150,35	4,72	0,164	0,106	0,0025	0,249	0,0012
22-23	95s	0,04	240,56	7,55	0,301	0,353	0,0028	0,203	0,0010
20-23	185s	0,38	390,92	12,27	0,164	0,106	0,0406	1,535	0,0077
20-24	185s	5,02	3.307,76	103,79	0,164	0,106	39,7099	171,602	0,8580
24-25	185s	0,15	3.307,76	103,79	0,164	0,106	1,1866	5,128	0,0256
25-26	185s	0,48	3.307,76	103,79	0,164	0,106	3,7970	16,408	0,0820
26-STATIE	185s	0,60	3.307,76	103,79	0,164	0,106	4,7462	20,510	0,1026
Total losses (MWh)					**57,56**				

One of the fundamental advantages of replacing overhead power lines (OHL) with underground cables (UGC) lies in the reduction of energy losses and the improvement of the voltage profile within distribution networks. This conversion enhances energy efficiency by limiting the exposure of conductors to external factors such as wind, rain, atmospheric corrosion, and extreme weather conditions—factors that can negatively impact the efficient transmission of electricity in the case of overhead lines.

Cables, due to their protected installation environment, benefit from superior thermal stability and increased durability compared to overhead lines, which leads to a lower risk of faults and a reduction in maintenance intervention frequency. However, the installation of underground networks involves high initial costs, and in the event of faults, fault localization and repair operations are more complex and expensive than for OHL systems.

From a technical standpoint, the conversion from OHL to UGC results in a significant reduction of active energy technical losses and an improved voltage profile, thereby contributing to the overall stability and efficiency of the distribution system. The analyses conducted within this study indicate a decrease in annual technical losses (CPT) from 146.46 MWh for the overhead line to only 57.56 MWh in the underground cable configuration. This difference represents a substantial 60.7% reduction in energy losses, which also corresponds to a noticeable decrease in voltage drop along the line.

In addition to the technical and economic benefits, the OHL–UGC conversion contributes to sustainability and environmental protection goals, aligning with European strategies for the energy transition. It is also relevant to note that, on an annual basis, the costs associated with loss reduction (CPT) are, on average, lower than those related to developing new primary energy sources, underlining the investment efficiency of such measures.

In this context, the implementation of UGC solutions with optimally sized conductors can represent a strategic alternative for network modernization, supporting both operational performance and environmental objectives.

4. INFLUENCE OF RENEWABLE SOURCES ON ELECTRICITY DISTRIBUTION SYSTEMS

4.1 Design of Electrical Installations for Active Users (Prosumers)

The integration of local renewable energy sources, particularly photovoltaic (PV) systems, into the electrical infrastructure of end-users for powering their own loads represents a strategic solution both for reducing pollution and for increasing energy efficiency [4.13]. This trend is becoming increasingly common, both in new installations and in modernized electrical systems.

Over the past decades—up to the 2020s—a visible transition has occurred from the classical model of a consumer supplied exclusively from a centralized generation system (possibly with a backup generator) toward complex and flexible architectures, found in commercial, industrial, and residential environments alike [4.13].

The initial phase of this transition was marked by the installation of photovoltaic panels on the rooftops of residential, commercial, and industrial buildings, connected directly to the public distribution network, in accordance with normative requirements such as IEC 60364-7-712 [4.14]. First published in 2002 and revised in 2017, this section specifies the technical requirements for PV installations.

Subsequently, PV generation has been increasingly integrated into consumers' internal electrical networks, primarily for self-consumption, often in combination with battery energy storage systems (BESS) to enhance resilience and flexibility [4.15].

This reconfiguration of installation architecture is strongly influenced by national and regional tariff policies. When the price of energy injected into the grid is lower than the tariff paid for energy consumed from the grid, self-consumption becomes the most economically advantageous option (see Fig. 4.1) [4.16].

This paradigm shift transforms the traditional electrical installations of passive consumers into active-user systems, characterized by the dual role of both producer and consumer of electrical energy.

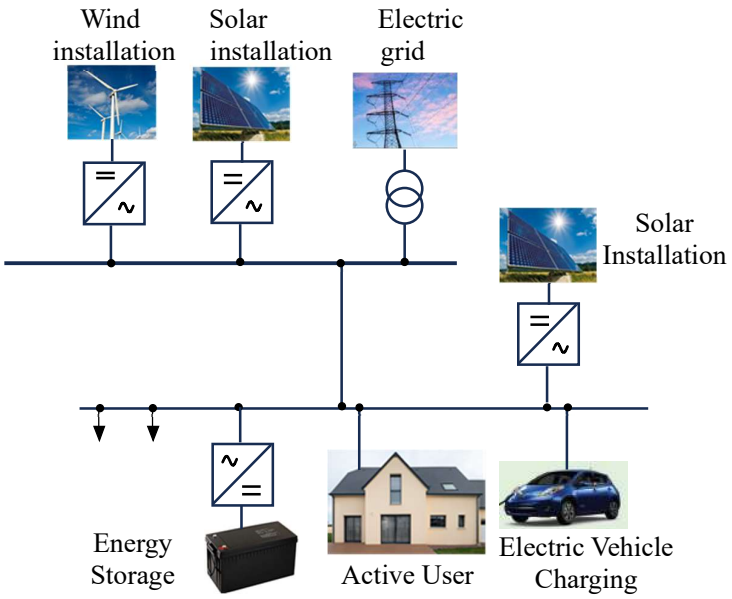


Fig. 4.1 – Example of an Active User (Prosumer) Electrical Installation Integrating Photovoltaic (or Wind) Energy Production, Self-Consumption, Storage, and EV Charging

According to international standards, the following definitions are used [4.13]:

- Active user (electrical installation) – "a network user that both consumes and produces electrical energy" [IEV 617-02-2];
- Microgrid – "an interconnected group of loads and distributed energy resources within clearly defined electrical boundaries, acting as a single controllable entity and capable of operating either in grid-connected mode or islanded mode. This definition includes both utility-owned distribution microgrids and customer-owned microgrids" [IEV 617-04-22].

According to international standards, the following definitions are used [4.13]:

- Active user (electrical installation) – "a network user that both consumes and produces electrical energy" [IEV 617-02-2];
- Microgrid – "an interconnected group of loads and distributed energy resources within clearly defined electrical boundaries, acting as a single controllable entity and capable of operating either in grid-connected mode or islanded mode. This definition includes both utility-owned distribution microgrids and customer-owned microgrids" [IEV 617-04-22].

4.2. Self-Consumption – Definition and Implications

Self-consumption of energy from local renewable sources, such as photovoltaic solar energy, represents an economic model in which the active user consumes the electrical energy generated internally to cover their own load demand. Thus, the active user simultaneously fulfills the roles of producer and consumer.

In the 2020s, self-consumption has become the preferred economic model due to the following key advantages:

- it offers, or will soon offer, greater economic benefits and enhanced control over energy bills;
- it allows the use of locally generated renewable energy, contributing to pollution reduction;
- it provides greater independence from the grid and protection against future fluctuations in electricity prices [4.15], [4.16].

It is also possible to add additional energy sources or storage systems (batteries), allowing operation in islanded mode (disconnected from the distribution network), as illustrated in Figure 4.3.

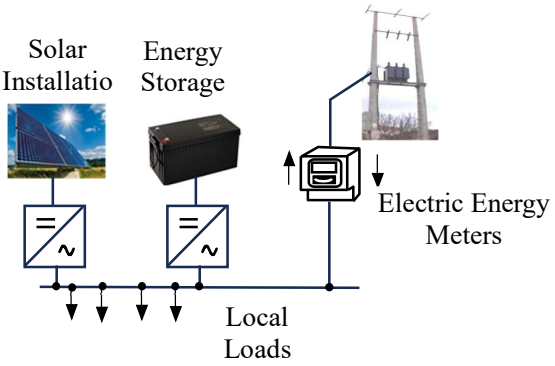


Fig. 4.3 Photovoltaic Generation and Energy Storage Used for Self-Consumption in Islanded *(Off-Grid)* Mode.

Technical Considerations in the Design of Electrical Installations with Integrated Photovoltaic Generation

The integration of photovoltaic (PV) energy into an active user's installation requires analysis of the following aspects:

- The connection point of the photovoltaic generation system within the installation;
- Determination of system parameters, including power balance between sources and loads;
- Sizing of the installation based on estimated generation and consumption profile;
- Protection of the installation against overvoltage, overcurrent, and unintended islanding operation;
- The energy management strategy, including coordination between PV generation, storage equipment, and supplied loads [4.15], [4.16].

4.3 Interaction Conditions with the Distribution Network for Active User Installations

The interaction conditions between an active user installation (Prosumer) and the distribution network are defined by national and European grid codes as well as specific technical standards [4.2], [4.17].

If a loss of the supply network occurs or if power quality parameters (such as voltage or frequency) deviate beyond permissible limits, no local generation source must remain connected to the network. This fundamental principle ensures the safety of the distribution system operator (DSO) personnel and prevents the risk of unintended energization of a faulty network [4.17].

In the event of a network outage, local sources (e.g., PV systems or storage units) must automatically disconnect. Although this measure may seem counterintuitive, it meets strict operational safety and electric shock protection requirements. Moreover, without dedicated design for islanded operation, a standard electrical installation cannot ensure the technical conditions required for autonomous operation, and its protection systems cannot be considered reliable [4.17].

4.4 Sizing of Electrical Installations with Solar Generation

All equipment within electrical installations must be sized considering all operating modes and the most severe constraints.

- Cables and busbars are dimensioned based on the maximum load current;
- Transformers are sized according to maximum power flow;
- Protection and switching devices are selected considering both maximum load current and minimum/maximum short-circuit currents [4.26].

When the photovoltaic generation capacity is lower than the energy demand, the impact on electrical installation sizing is negligible or nonexistent:

- The current flow through cables and busbars does not increase with the addition of PV generation;
- The transformer power flow decreases due to PV contribution.

When the photovoltaic generation capacity exceeds the energy demand, the impact on electrical design must be carefully evaluated, as current and power flows in the installation may increase.

For new constructions, higher power and current constraints are addressed during the early design phase, allowing proper sizing of the installation. However, for existing users, the following aspects should be considered:

- Connecting the PV system upstream of the main busbar avoids the need for modifications in the main switchboard;
- Using a PV output control system can prevent the need to replace the transformer and its protection devices [4.17].

4.5 Electrical Energy Storage Systems (EES)

Electrical Energy Storage Systems (EES) are a key component of modern power networks, contributing to balancing supply and demand, integrating renewable sources, and optimizing the operation of the energy infrastructure. These systems can store available energy at a given time and release it later, according to network or end-user needs [4.27].

Due to their technological and functional diversity, EES solutions vary significantly in capacity, response time, lifetime, and energy efficiency. The main storage categories include:

- Electrochemical batteries,
- Pumped hydro storage (PHS),
- Thermal storage systems,
- Gas-based storage (e.g., hydrogen or methane),
- Capacitors and supercapacitors [4.28].

The applications of storage systems are manifold:

- peak load reduction,
- compensation of renewable generation variability (arbitrage service),
- provision of ancillary services for frequency and voltage regulation,
- reduction of network losses,

- enhancement of grid resilience and reliability [4.29], [4.30].

Thus, the implementation of these technologies is fundamental for the transition toward a flexible, intelligent, and sustainable energy system. Storage systems enable dynamic control of power flows, contributing to pollution reduction and efficient utilization of available energy resources [4.31].

4.5.1 Impact of Energy Storage Systems on Electrical Infrastructure

Energy storage systems positively influence electrical infrastructure in several ways:

- Network optimization: By reducing peak loads, EES systems decrease transformer and transmission line loading, delaying or avoiding the need for infrastructure expansion [4.30].
- Grid stabilization: They provide ancillary services such as real-time frequency and voltage regulation, ensuring high power quality [4.29], [4.37].
- Loss reduction: Locally stored energy can be used to supply nearby loads, avoiding long-distance transport and reducing Joule losses [4.32].
- Renewable integration: Storage systems compensate for the intermittency of wind and solar sources, enhancing energy stability and maximizing renewable utilization [4.31], [4.35].
- Operational cost reduction: By enabling consumption flexibility and reducing the need for peak power plants, EES systems help lower network operating costs [4.38].

4.6 Case Study

Figure 4.15 illustrates a relevant case study aimed at evaluating the integrated effects of connecting an active user to the distribution network. In this scenario, at point 6 of the scheme, an active user with an installed power of 350 kW was connected. The analysis highlights a series of notable technical benefits resulting from this connection, including the reduction of energy losses in the targeted area, decrease of voltage drops, and improvement of the power quality delivered to downstream consumers.

It can be observed that local energy injection into the network contributes to an increase in the voltage level at the connection point, which implicitly leads to a higher available power for users in the area. This improvement in the voltage profile has a positive effect on the reliability and quality of supply—essential aspects in a modern electrical system oriented toward distributed generation integration.

At the same time, the study emphasizes the importance of conducting detailed analyses to support decisions regarding the integration of new active users into existing networks. It is essential to assess the network's behavior with respect to voltage variations induced by the intermittent operation of the active user, especially during time intervals when no energy is injected into the grid (e.g., at night). This allows for an accurate determination of the integration limits of distributed sources and ensures compliance with voltage quality standards at user terminals.

Therefore, such simulations and impact assessments must be an integral part of the planning and sizing process for intelligent distribution networks, supporting the sustainable integration of active users and the development of a flexible and resilient energy system.

The analysis revealed that using an underground power line (UGC) to supply active users in a rural medium-voltage (20 kV) network provides superior performance compared to the traditional overhead line (OHL) solution. This construction approach not only improves voltage quality and reduces energy losses, but also proves effective in

managing power flows, particularly in situations involving reverse power flow phenomena caused by the integration of active users or distributed renewable sources.

Thus, the implementation of underground cable networks in rural areas can help mitigate the negative effects of reverse power flows, ensuring more stable and predictable operation of the distribution system. Moreover, this solution enhances the adaptability of the network to the new requirements imposed by the energy transition and the increasing level of electrification in rural environments.

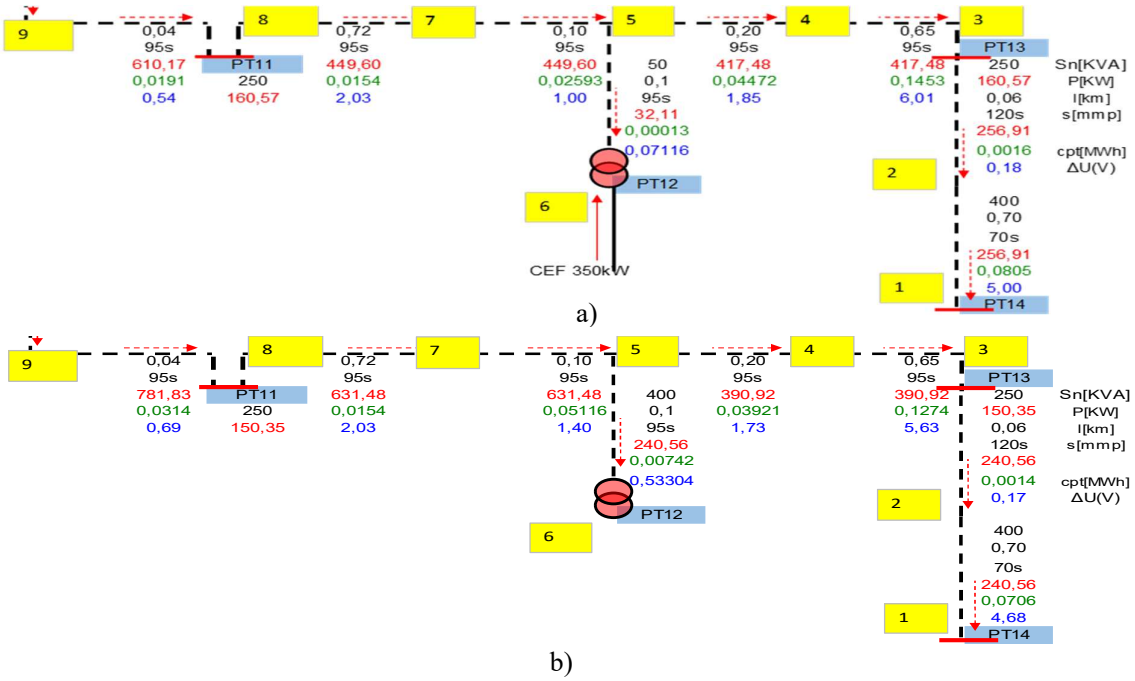


Fig. 4.15 Comparative Analysis of the Scheme Characteristics with an Active User Connection: a) active user in operation; b) inactive (disconnected) user.

5. REVERSE POWER FLOW

In situations where the share of Distributed Energy Resources (DER) becomes significant relative to the local load, a phenomenon known as reverse power flow can occur. This condition is characterized by the injection of energy from the distribution network into the transmission network, a shift that affects both system planning and operation [5.6], [5.8].

This new operating paradigm highlights the strategic importance of interconnection transformers, which play a crucial role in regulating power flows and maintaining balance between different network levels [5.2], [5.7]. Adapting equipment and control schemes is essential to ensure an efficient transition toward a flexible, resilient, and environmentally sustainable power system [5.5], [5.9].

The circulation of reverse power flows is a complex phenomenon of growing significance in the current context of the global energy transition [5.2–5.8]. This phenomenon arises when locally generated electricity, particularly from distributed renewable sources, exceeds the instantaneous consumption of users in a given area, resulting in a power flow opposite to the traditional direction — that is, from the

distribution network toward the transmission network or toward other nodes within the grid.

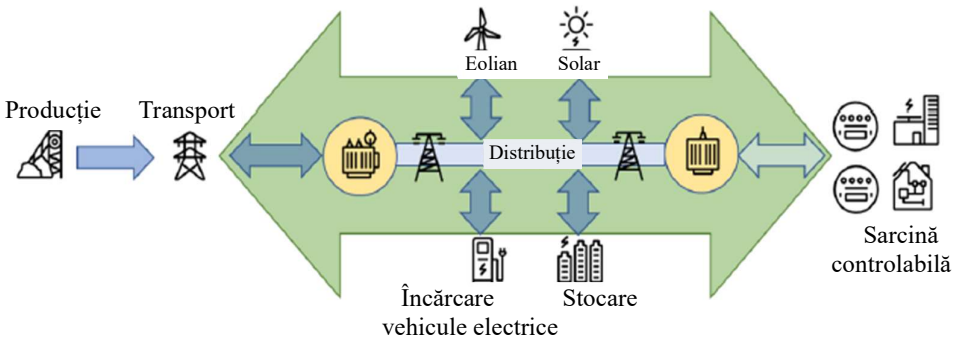


Fig. 5.1 Structure of a Future Electrical Energy Transmission System..

5.2 Reverse Power Flow in Distribution Networks – Causes, Effects, and Operational Implications

Reverse power flow is a phenomenon of growing importance in the context of the energy transition and the rapid penetration of distributed renewable sources. It refers to the circulation of electrical energy from consumption points or local generators (active users) toward the electrical network, thereby reversing the traditional direction of power flow—from the transmission and distribution grid to end users [5.4].

The occurrence of reverse power flow is directly linked to technological progress and the increasing integration of renewable energy sources, particularly photovoltaic (PV) systems installed at household, commercial, or community levels. In this context, the study analyzed the root causes, conditions of occurrence, and systemic effects of this phenomenon, as well as the potential control and infrastructure adaptation measures required for its efficient management.

Generally, reverse power flows are most frequently encountered in urban and suburban networks, characterized by high user density and relatively long distribution lines. In these areas, a significant proportion of consumers are equipped with solar generation systems, capable of injecting energy into the grid whenever local production exceeds self-consumption [5.11], [5.12].

The theoretical power generated by a solar installation that includes photovoltaic panels with an area A_{PV} and efficiency k_{PV}, under a solar irradiance G, is given by the following relation:

$$P_{PV} = k_{PV} \cdot A_{PV} \cdot G \cdot \qquad (5.1)$$

Given the specific shape of the photovoltaic system generation curve, which varies significantly depending on atmospheric conditions, as well as the consumption profile curve of users (Fig. 5.2), there are time intervals during which the generated power P_{PV} exceeds the locally required power.

In the absence of an efficient mechanism for redistributing the surplus energy to other consumers or to storage systems, the excess energy is fed back into the distribution network, generating a reverse power flow on a local or extended scale.

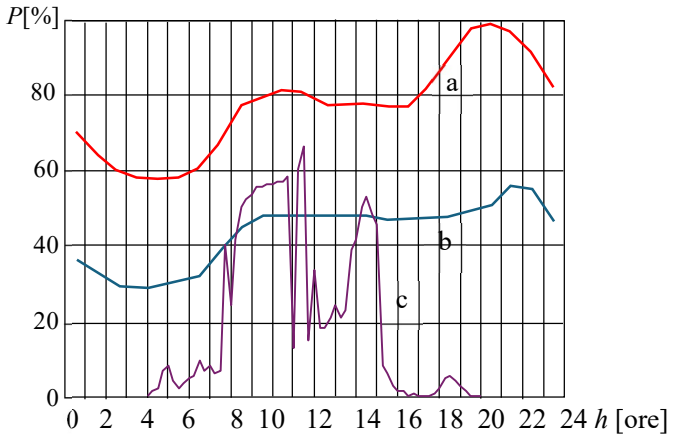


Fig. 5.2 Typical Load Curve of a User on a Winter Day (a), on a Summer Day (b), and Energy Generated by the Solar Installation on a Cloudy Summer Day (c).

Figure 5.3 presents the load curve of a 630 kVA distribution transformer, representative of a rural environment with a high number of active users connected to the network [5.13].

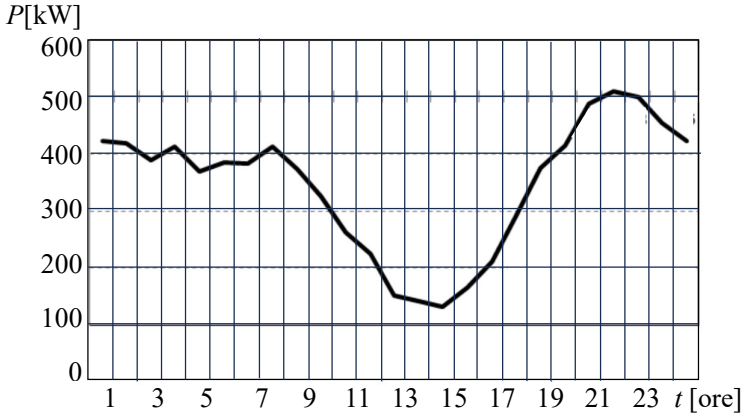


Fig. 5.3 Variation of the Transformer Loading Due to Reverse Power Flow During Midday Hours.

In this analysis, it is considered that during the operating interval of the photovoltaic sources, the total power P_T flowing through the supply transformer is determined by the following relation:

$$P_T = P_s - P_{PV} \tag{5.2}$$

When:

P_T - represents the active power flowing through the distribution transformer;

P_S - represents the total load of connected users, including the active losses of the network;

;

P_{PV} - represents the active power generated locally by the photovoltaic systems connected to the network [5.14].

This relationship clearly illustrates how local generation reduces the effective load on the transformer and can even reverse the direction of power flow. When $P_{PV} > P_S$, the resulting P_T becomes negative, reflecting a reverse power flow from the low-voltage network toward the medium-voltage network.

This behavior has direct implications on the sizing, protection, and operation of network equipment and requires a reconsideration of power system operation strategies, particularly in regions with a high penetration of distributed renewable sources.

5.3 Effects of Reverse Power Flow

The extensive integration of Distributed Energy Resources (DER), particularly those based on electronic conversion, causes substantial changes in the operation of electrical networks. Among the most notable consequences is the emergence of reverse power flow, which has a direct impact on the network infrastructure, operational economy, and control processes.

5.3.1 Technical Effects

a) **Equipment Overloading**. Transformers and power lines in distribution networks are traditionally designed to support unidirectional energy flows. The reversal of this flow can lead to:

- **Increased Joule losses,** due to current redistribution in conductors and transformer windings [5.15];
- **Overheating of equipment,** leading to accelerated insulation degradation and reduced service life;
- **Exceeding nominal capacities of components,** particularly during simultaneous injections from multiple prosumers.

b) **Voltage and Frequency Fluctuations.** The injection of active and reactive power into the main grid can disturb the nominal operating parameters of the system:

- **Local overvoltages**, caused by excessive generation at weakly connected nodes;
- **Frequency oscillations**, especially in isolated or weakly interconnected systems, affecting sensitive equipment and overall system stability.

c) **Protection Malfunctions**. Conventional protection systems (e.g., overcurrent, directional, or distance relays) are configured to detect faults assuming unidirectional current flow. Reverse current flow may result in:

- **Fault misinterpretation**, leading to incorrect tripping actions;
- **Failure to detect actual faults**, especially when DER injection occurs near the fault location [5.16].

d) **Harmonics and Power Quality Degradation.**The use of inverters for renewable integration (PV, batteries, etc.) introduces higher-order harmonics, affecting:

- **Voltage stability and control within the network**;
- **Performance of electronic devices**, which are susceptible to harmonic distortion [5.17].

5.3.2 Economic Effects

a) Reduction of Energy Efficiency. Reverse flows and network imbalances generate additional losses, reducing the overall system efficiency:

– Increased losses in transformers and lines;

– **The need for more frequent maintenance,** leading to significantly higher operational costs.

b) Metering and Billing Issues. In the absence of bidirectional smart meters:

- The calculation of delivered and absorbed energy becomes inaccurate or ambiguous;
- Financial losses may occur for either the operators or the active users, depending on the metering configuration.

c) Need for Additional Investments. Adapting the network to handle bidirectional power flows requires:

- Modernization of protection and control equipment;
- Reconfiguration and digitalization of the network topology;
- Significant capital investments by system operators [5.18].

5.3.3 Operational Effects

a) Increased Operational Complexity. Managing reverse power flows requires a high degree of operational flexibility:

- Continuous real-time monitoring of the network state;
- Advanced power flow control algorithms to optimize power distribution based on local and global conditions.

b) Risk of Outages and Faults. Without proper control, unplanned reverse flows can cause:

- **Local overloads**, resulting in accidental equipment tripping;
- **Unintended interactions between DER units and the grid**, leading to instability and disturbances in power supply continuity..

5.4 Impact of Reverse Power Flow on Transformer Performance According to Operating Quadrants

In the current context of the energy transition, characterized by the extensive integration of distributed energy resources (DER) and the growing number of active users, distribution network transformers are subjected to operational conditions significantly different from their conventional operating regime. The reverse power flow regime fundamentally alters the transformer's operating parameters, especially when it operates across the four quadrants of power flow, defined according to the direction of active (P) and reactive (Q) power. This section provides a detailed analysis for each quadrant, examining the technical performance impact on the transformer, supported by illustrative examples and operational considerations.

Power flows in electrical networks can be analyzed and classified into four functional quadrants (Q1–Q4), based on the sign of the active power (P) and reactive power (Q) (Fig. 5.4).

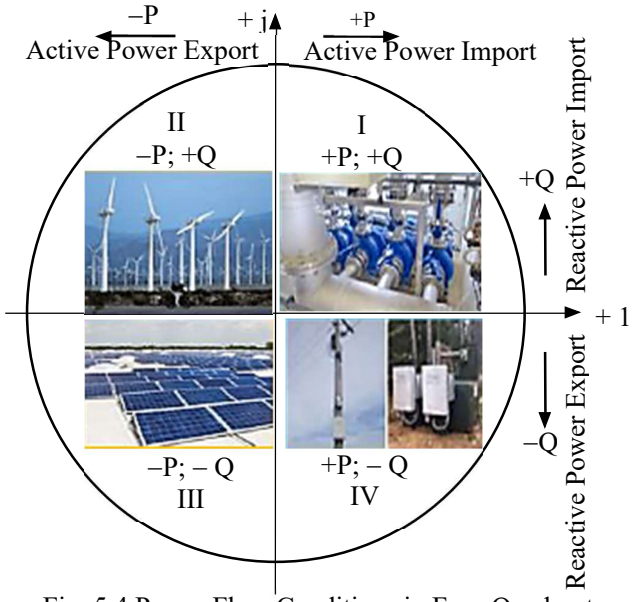


Fig. 5.4 Power Flow Conditions in Four Quadrants.

As previously discussed, the magnetizing flux in the ferromagnetic core of a transformer is determined by the excitation voltage (E). This voltage varies depending on the transformer's position within the active–reactive power diagram quadrants, as follows:

- **Quadrants Q1 and Q2**: the excitation voltage is supplied by the electrical network (direct flux);
- **Quadrants Q3 and Q4**: the excitation is provided by distributed energy sources (reverse flux).

In operating regimes Q3 and Q4, characterized by reverse power flow, the excitation voltage tends to exceed the design limits of the transformer, as it overlaps with a secondary-side voltage U_2 already elevated—often set about 5% above the nominal value to compensate for voltage drops along the feeder [5.21]. Consequently, the magnetic flux in the core increases significantly, surpassing the optimal operating point of the magnetization curve, which leads to a sharp rise in both the magnetizing current and iron (core) losses.

Final considerations:

- The Q3 and Q4 regimes are the most demanding, requiring transformers designed for bidirectional power flow, equipped with integrated thermal and harmonic monitoring;
- The protection and control systems must be reconfigured to prevent false tripping under reverse-flow conditions;
- Real-time analysis of transformer currents and voltages, using smart sensors and AI-based algorithms, can prevent premature equipment degradation.

Therefore, the design, operation, and maintenance of transformers in modern networks must explicitly consider the four-quadrant operating conditions, with a strong focus on safety, reliability, and adaptability.

6. DIMENSIONING OF A HIGH-POWER (6 MW) CHARGING STATION AND ITS IMPACT ON THE ELECTRICITY DISTRIBUTION SYSTEM

6.1. Charging Station

The expansion of electric transportation for heavy-duty vehicles has led to the design of charging stations equipped with 10–12 charging points, which operate at installed capacities of 1.5–1.8 MW, thus requiring direct connection to the medium-voltage network [6.4], [6.9].

A fast-charging station (AC/DC) connected to the medium-voltage grid consists of the following main components:grid harmonic filters, high-power rectifier, power factor control unit, DC/AC converter that generates a medium-frequency voltage (≈10 kHz) at the isolation transformer terminals, medium-frequency rectifier, output filter, and output terminals for the supply cable, as illustrated in Figure 6.2 [6.5], [6.10].

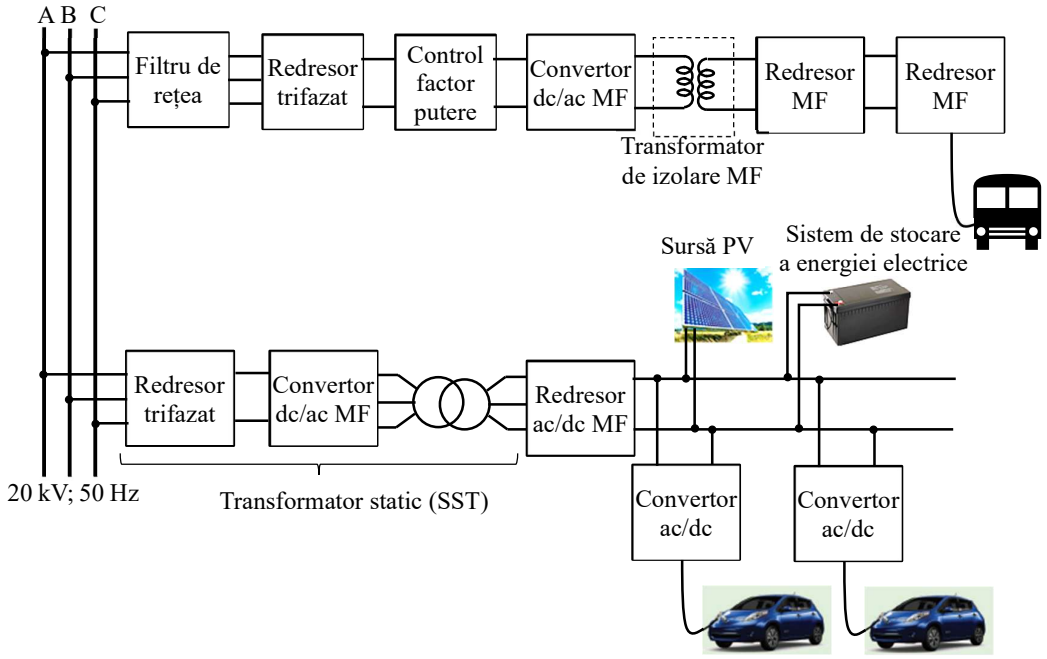


Fig. 6.2 – Schematic diagram of an electric vehicle charging station supplied from the medium-voltage network, comprising a high-power and fast-charging section, as well as a section dedicated to passenger vehicle charging

To rival the performance of conventional liquid-fuel stations, modern electric vehicle charging stations include both a high-power fast-charging section and a dedicated section for passenger vehicle charging, supplied through a Solid-State Transformer (SST) [6.4]. The integration of SSTs provides several advantages, such as: reduced footprint, lower power losses, optimized investment costs, and mitigation of fire hazards [6.9].

In addition, photovoltaic (PV) sources and energy storage systems can be connected to the DC busbars of the station, thus contributing to the integration of renewable energy sources [6.2].

The three-phase power supply of the station eliminates the risk of current imbalance, thereby reducing disturbances caused by asymmetrical loading. Under these conditions, network disturbances mainly originate from the nonlinear behavior of power electronic equipment and from voltage fluctuations associated with the connection and disconnection of high-power vehicles [6.6], [6.8].

The power factor control system of the station ensures compliance with the limits imposed by the distribution system operator (DSO), thus preventing issues related to reactive power flow [6.7].

To limit the level of harmonics generated by the three-phase rectifier, semiconductor switching is controlled using Pulse Width Modulation (PWM) [6.5]. The harmonic levels are maintained within the limits defined by international standards, thanks to both the control scheme and the grid filters [6.8].

The disturbance analysis must consider not only the background disturbances of the supply network but also the short-circuit power at the connection node [6.9].

The isolation transformer provides electrical separation between the vehicle and the distribution network, preventing any accidental grounding of the electric vehicle battery [6.10].

The charging process is generally carried out in two stages:

- initially, at constant current (C), during which the voltage at the battery terminals gradually increases;
- subsequently, at constant voltage (V), during which the current gradually decreases, and the power drawn from the grid is correspondingly reduced (Fig. 6.3) [6.1], [6.3].

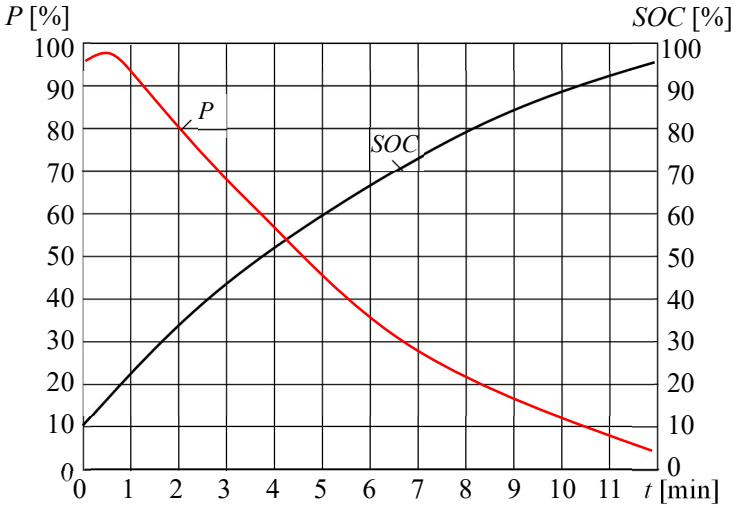


Fig. 6.3 – Variation of absorbed power (P) and battery terminal voltage (SOC) during the charging process.

Figure 6.4 presents a two-stage charging strategy consisting of an initial constant current (CC) phase followed by a constant voltage (CV) phase. The process begins with the application of a constant charging current until a predefined voltage value—known as the cut-off voltage—is reached [6.11], [6.12].

For Li-Ion batteries equipped with conventional cathode materials such as cobalt, nickel, manganese, or aluminum, the standardized cut-off voltage is approximately 4.20 V per cell, with a tolerance of ±50 mV per cell [6.13]. Once this threshold is achieved, the charging process continues under constant-voltage conditions, maintaining the voltage at the defined level.

Charging is considered complete when the current decreases to a level between 3% and 5% of the cell's nominal current [6.14]. It is important to emphasize that maintenance charging strategies (such as trickle charge or float charge), commonly used for other types of batteries, are not compatible with Li-ion technology. Applying these methods can lead to the deposition of metallic lithium on the electrodes, a phenomenon that compromises both the safety and structural integrity of the cell [6.15], [6.16].

As an alternative, a topping charge is recommended, applied only when the voltage drops below a predefined threshold. This approach allows the long-term preservation of the cell's capacity without introducing additional risks to operational safety [6.17].

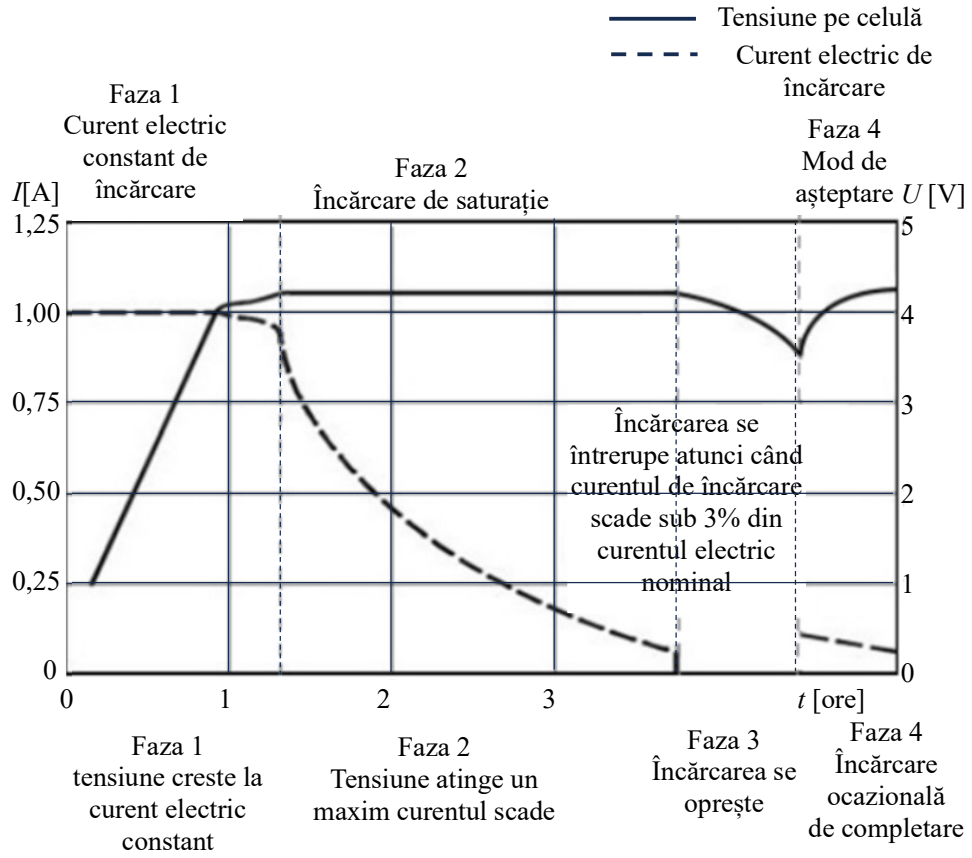


Fig. 6.4 C–V charging stages for a Li-ion battery

Diversity Factor and EVCS Sizing

For an accurate estimation of the required power, it is essential to consider the temporal variation of load peaks associated with clusters of charging stations. The study [6.20] demonstrated that the diversity factor depends mainly on the number of electric vehicles, and to a lesser extent on the number of charging points. According to the analysis, this factor decreases rapidly to approximately 0.3 when the number of vehicles exceeds 30, and can drop below 0.25 for more than 50 electric vehicles.

Similar results were reported in [6.6], where it was found that for 100 charging stations, the maximum diversity factor ranged between 0.3 and 0.4, while for 1000 stations, the value decreased to around 0.2 [6.23]. These findings highlight the crucial role of this parameter in EVCS modeling and planning, enabling more efficient use of resources and minimizing the risk of network overloading [6.24].

Mathematically, the diversity factor (FD**)** is defined as:

$$FD = \frac{\sum_{i=1}^{n} D_i}{D_{max}}, \tag{6.6}$$

where:

- *Di* represents the individual maximum demand of load *i* ;
- *Dmax* –represents the maximum simultaneous demand of the entire system.

6.5 Case Study

Within this research, the feasibility of supplying electric power to a highway fast-charging station was analyzed, as shown in Figure 6.10. The station is equipped with 14 high-power fast-charging points designed for both electric vehicles and electric trucks. The total installed capacity of the charging hub is approximately 6 MW, and the facility is located along a highway, about 20 km from the nearest 110/20 kV primary substation.

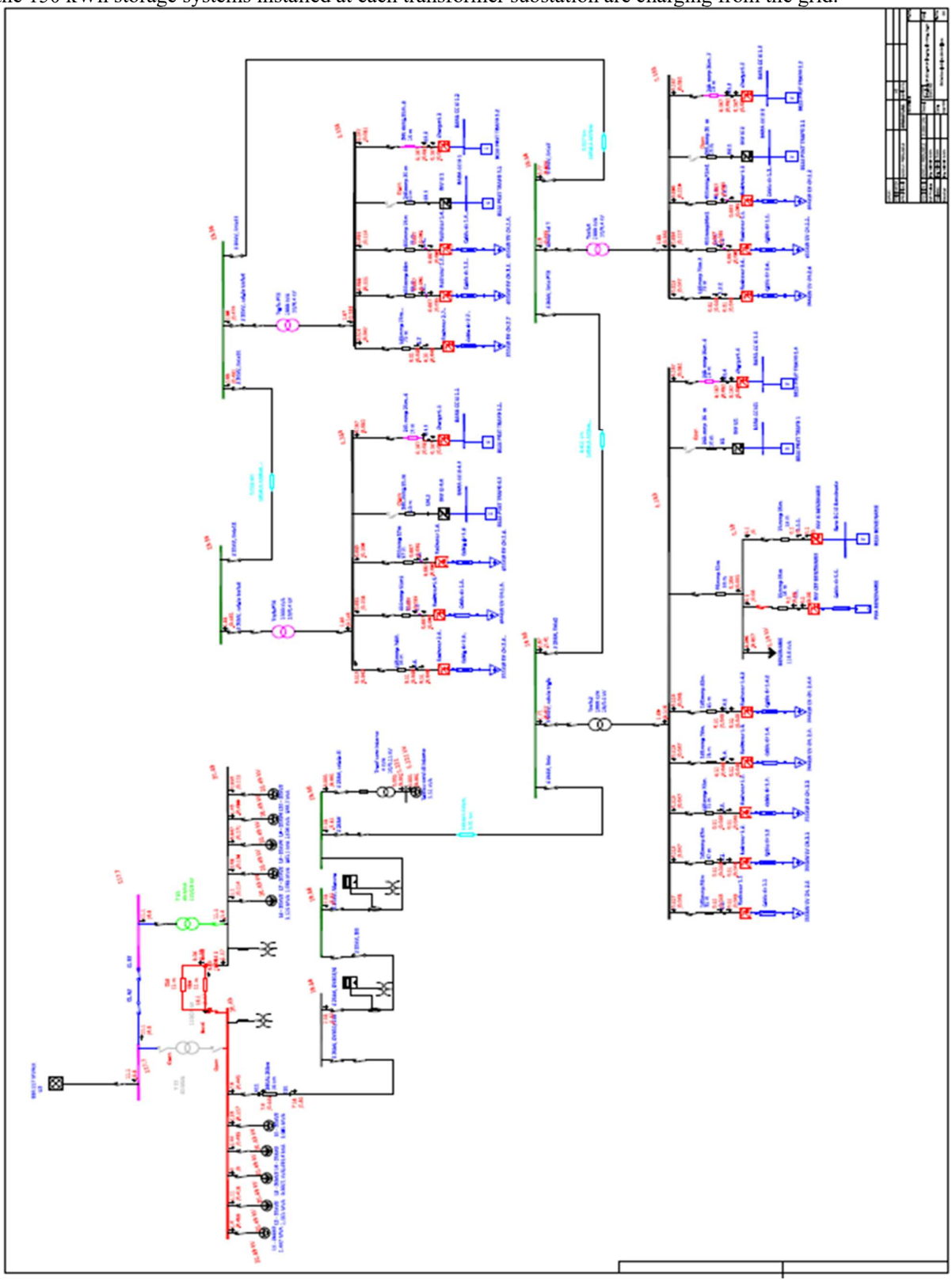
The project also considered the integration of a 200 kW photovoltaic plant and an energy storage system with a capacity of 600 kWh, in order to increase the level of local self-consumption and to reduce the impact on the distribution network.

The charging infrastructure is designed to allow the simultaneous use of 8 electric cars and 6 electric trucks. Each charging point dedicated to passenger vehicles has a rated power of 300 kW, ensuring a full battery recharge within 15–20 minutes. In the case of electric trucks, the stations are rated at 600 kW, capable of completing a full charge within 1–1.5 hours. By comparison, low-power charging infrastructure, with capacities below 25 kW, requires several hours—typically overnight—to complete the charging process.

Four operational scenarios were analyzed in this thesis:

- Scenario 1: All charging stations are connected, and each 150 kWh storage system installed at the transformer substations operates in charging mode from the grid, as shown in Figure 6.11.
- Scenario 2: All charging stations are connected, and each 150 kWh storage system installed at the transformer substations operates in discharging mode, injecting energy into the grid, as shown in Figure 6.12.
- Scenario 3: All 300 kW charging stations are disconnected, the 600 kW stations remain connected, and each 150 kWh storage system at the transformer substations operates in charging mode from the grid, as shown in Figure 6.16.
- Scenario 4: All 300 kW charging stations are disconnected, the 600 kW stations remain connected, and each 150 kWh storage system at the transformer substations operates in discharging mode, injecting energy into the grid, as shown in Figure 6.17.

Fig. 6.11 Case study illustrating the situation where all charging stations are connected, and the 150 kWh storage systems installed at each transformer substation are charging from the grid.



Following the simulations and calculations performed using the ETAP software, the following values were obtained (Tables 6.1 and 6.2).

Table 6.1 Voltage drop calculation and active and reactive power losses for the case in which all charging stations are connected and the 150 kWh storage systems installed at each transformer substation are charging from the grid.

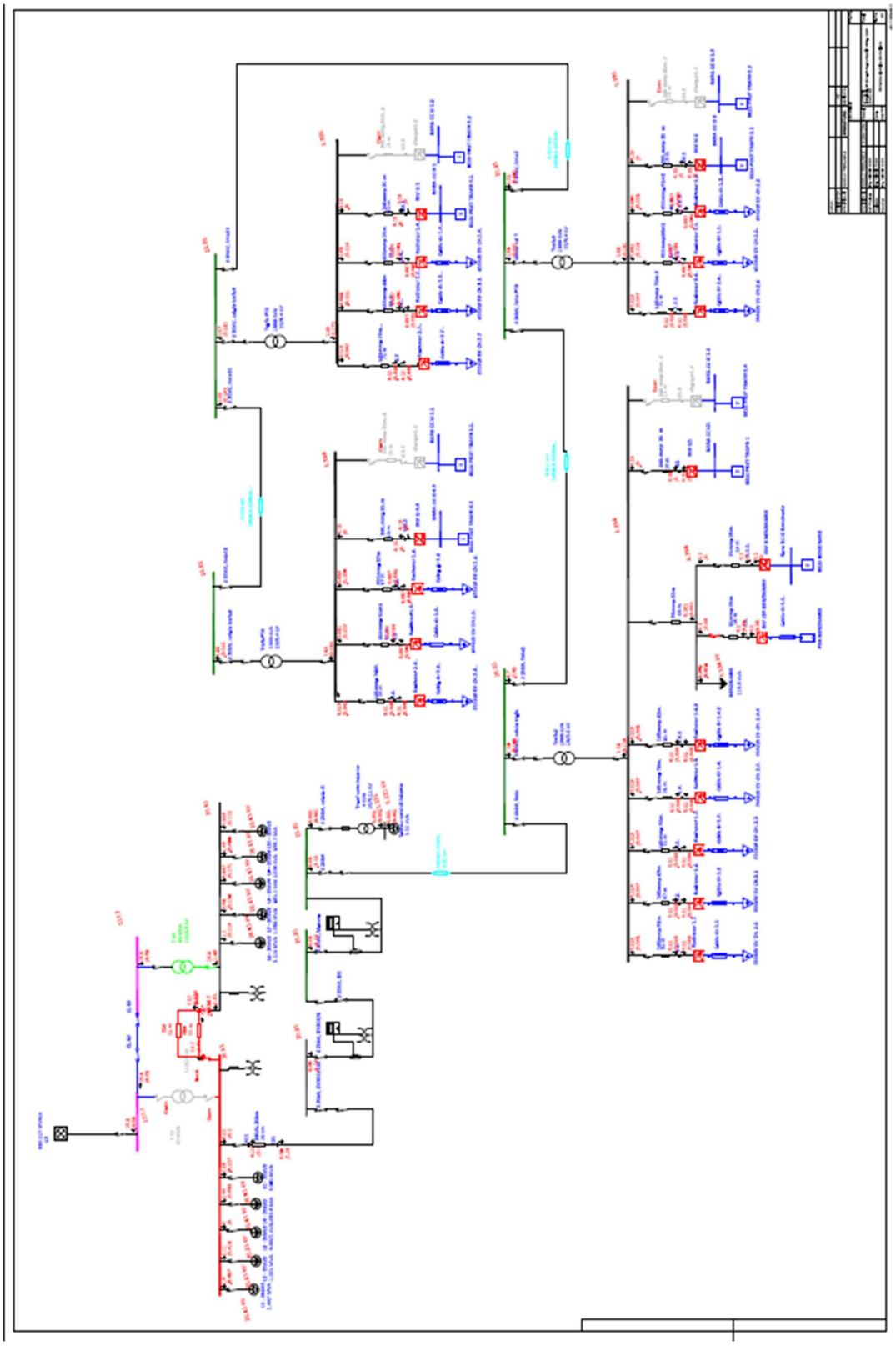
Network Element	From	To	Length [m] / Transformation ratio [kV]	Voltage drop [%]	Active power losses [kW]	Reactive power losses [kvar]
70mmp 35m	0.0.	BARA TDJT BENZINARIE	35 m	0,29	0,291	0,0387
70mmp 35m.	0.0.0.	BARA TDJT BENZINARIE	35 m	0,29	0,291	0,0387
95mmp 50m	BARA TDJT BENZINARIE	Bara PT1	50 m	0,27	0,405	0,0713
185AL0.02km.	Compartiment Benefic	Post trafo 1 - 2000kVA	20 m	0,01	0,24	-0,558
185AL0.032km...	Post trafo 1 - 2000kVA	Post trafo 2 - 2000kVA	32 m	0,01	0,367	-0,902
185AL0.037km-	Post trafo 2 - 2000kVA	Post trafo 3 - 2000kVA	37 m	0,01	0,187	-1,17
185AL0.038km..-	Post trafo 3 - 2000kVA	Post trafo 4- 2000kVA	38 m	0	0,0477	-1,28
240 mmp 20m..4	Bara PT4	IS 1.1	20 m	0,41	0,682	0,362
240 mmp 20m..6	Bara PT3	IS1.2	20 m	0,41	0,683	0,362
240 mmp 20m..7	Bara PT2	IS1.3	20 m	0,41	0,683	0,362
240 mmp 20m..8	Bara PT1	IS1.4	20 m	0,41	0,664	0,352
240AL 20km	011	010	20000 m	1,96	86,52	-1502,2
400mmp 51m1	Bara PT4	1.5	51 m	2,43	15,31	12,27
400mmp 57m	Bara PT4	1.6.	57 m	2,72	17,21	13,79
400mmp 68m	Bara PT3	1.3..	68 m	3,27	20,78	16,66
400mmp 75m	Bara PT3	1.4..	75 m	3,63	23,09	18,51
400mmp84m1	Bara PT2	1.1	84 m	4,09	26,13	20,94
400mmp 91m1	Bara PT2	1.2..3	91 m	4,45	28,52	22,86
Cb5	Bus3	Bus4	12 m	0	0,0513	0,131
Cb6	Bus3	Bus4	12 m	0	0,0513	0,131
T 10-P	Bara B 110kV3		110/20kV	4,28	23,73	1068
T 10-S	Bara B 20kV3		110/20kV	4,28		
Trafo PT3-P	Post trafo 3 - 2000kVA		20/0,4kV	1,86	13,03	78,15
Trafo PT3-S	Bara PT3		20/0,4kV	1,86		
Trafo2-P	Post trafo 1 - 2000kVA		20/0,4kV	0,47	0,127	0,763
Trafo2-S	Bara PT1		20/0,4kV	0,47		
Trafo4-P	Post trafo 2 - 2000kVA		20/0,4kV	1,9	13,24	79,42
Trafo4-S	Bara PT2		20/0,4kV	1,9		
TrafoPT4-P	Post trafo 4- 2000kVA		20/0,4kV	1,83	12,8	76,83
TrafoPT4-S	Bara PT4		20/0,4kV	1,83		
Tranf serv interne-P	Compartiment Benefic		20/0,23 kV	3	0,0627	0,094

Tranf serv interne-S	Tablou SI		20/0,23 kV	3		

Table 6.2 Voltage deviation calculation for the case in which all charging stations are connected and the 150 kWh storage systems installed at each transformer substation are charging from the grid.

Network Element	Nominal Voltage kV	Voltage deviation [%]
0.0.	0.4	100,85
0.0.0.	0.4	100,85
Bara A 20kV3	20	102,72
Bara A 110kV3	110	107
Bara B 20kV3	20	102,72
Bara B 110kV3	110	107
Bara PT1	0.4	100,29
Bara PT2	0.4	98,85
Bara PT3	0.4	98,88
Bara PT4	0.4	98,91
BARA TDJT BENZINARIE	0.4	100,55
Compartiment Benefic	20	100,76
Compartiment Benefic2	20	100,76
Compartiment ENEL	20	100,76
Post trafo 1 - 2000kVA	20	100,76
Post trafo 2 - 2000kVA	20	100,75
Post trafo 3 - 2000kVA	20	100,74
Post trafo 4- 2000kVA	20	100,74
Tablou SI	0,23	97,77

Fig. 6.12 Case study illustrating the situation where all charging stations are connected, and the 150 kWh storage systems installed at each transformer substation are discharging into the grid.



Following the simulations and calculations performed using the ETAP software, the following values were obtained (Tables 6.3 and 6.4).

Table 6.3 Voltage drop calculation and active and reactive power losses for the case in which all charging stations are connected and the 150 kWh storage systems installed at each transformer substation are discharging into the grid.

Network Element	From	To	Length [m] / Transformation ratio [kV]	Voltage drop [%]	Active power losses [kW]	Reactive power losses [kvar]
70mmp 35m	0.0.	BARA TDJT BENZINARIE	35 m	0,32	0,409	0,0544
70mmp 35m.	0.0.0.	BARA TDJT BENZINARIE	35 m	0,3	0,301	0,04
95mmp 50m	BARA TDJT BENZINARIE	Bara PT1	50 m	0,31	0,322	0,0568
185AL0.02km.	Compartiment Benefic	Post trafo 1 - 2000kVA	20 m	0,01	0,39	-0,467
185AL0.032km...	Post trafo 1 - 2000kVA	Post trafo 2 - 2000kVA	32 m	0,01	0,373	-0,885
185AL0.037km-	Post trafo 2 - 2000kVA	Post trafo 3 - 2000kVA	37 m	0,01	0,19	-1,15
185AL0.038km-	Post trafo 3 - 2000kVA	Post trafo 4- 2000kVA	38 m	0	0,0484	-1,27
185mmp 67m	Bara PT1	IS 1.1	67 m	1,46	4,68	1,6
185mmp 73m.	Bara PT1	IS1.2	73 m	1,6	5,11	1,75
185mmp 73m...	Bara PT3	IS1.3	73 m	1,6	5,14	1,75
185mmp 73m.2	Bara PT2	IS1.4	73 m	1,6	5,15	1,76
185mmp 76M.	Bara PT4	010	76 m	1,67	5,36	1,83
185mmp 78m.	Bara PT1	1.5	78 m	1,71	5,48	1,87
185mmp 83m.	Bara PT1	1.6.	83 m	1,82	5,84	1,99
185mmp 93m	Bara PT1	1.3..	93 m	2,04	6,58	2,24
240.mmp 20 m	IS2.1	1.4..	20 m	0,29	0,448	0,237
240.mmp 20 m	IS1	1.1	20 m	0,29	0,445	0,236
240.mmp 20.m	IS4.3	1.2..3	20 m	0,29	0,447	0,237
240AL 20km	011	Bus4	20000 m	2,51	143,8	-1452,9
240mmp 20 m	IS3.1	Bus4	20 m	0,29	0,447	0,237
400mmp 51m1	Bara PT4		51 m	2,44	15,48	12,41
400mmp 57m	Bara PT4		57 m	2,74	17,41	13,95
400mmp 68m	Bara PT3		68 m	3,29	21,02	16,85
400mmp 75m	Bara PT3		75 m	3,65	23,36	18,72
400mmp84m1	Bara PT2		84 m	4,11	26,44	21,19
400mmp 91m1	Bara PT2		91 m	4,47	28,86	23,13
Cb5	Bus3		12 m	0	0,0627	0,16
Cb6	Bus3		12 m	0	0,0627	0,16
T 10-P	Bara B 110kV3		110/20kV	4,34	27,28	1227,6
T 10-S	Bara B 20kV3		110/20kV	4,34	0	0
Trafo PT3-P	Post trafo 3 - 2000kVA		20/0,4 kV	1,78	13,21	79,25
Trafo PT3-S	Bara PT3		20/0,4 kV	1,78	0	0
Trafo2-P	Post trafo 1 - 2000kVA		20/0,4 kV	1,54	10,3	61,79
Trafo2-S	Bara PT1		20/0,4 kV	1,54	0	0

Trafo4-P	Post trafo 2 - 2000kVA		20/0,4 kV	1,81	13,42	80,53
Trafo4-S	Bara PT2		20/0,4 kV	1,81	0	0
TrafoPT4-P	Post trafo 4- 2000kVA		20/0,4 kV	1,74	12,99	77,92
TrafoPT4-S	Bara PT4		20/0,4 kV	1,74	0	0
Tranf serv interne-P	Compartiment Benefic		20/0,23 kV	3,01	0,0632	0,0948
Tranf serv interne-S	Tablou SI		20/0,23 kV	3,01	0	0

Table 6.4 Voltage deviation calculation for the case in which all charging stations are connected and the 150 kWh storage systems installed at each transformer substation are discharging into the grid.

Network Element	Nominal Voltage kV	Voltage deviation [%]
0.0.	0.4	99,24
0.0.0.	0.4	99,21
Bara A 20kV	20	102,66
Bara A 110kV	110	107
Bara B 20kV	20	102,66
Bara B 110kV	110	107
Bara PT1	0.4	98,6
Bara PT2	0.4	98,32
Bara PT3	0.4	98,35
Bara PT4	0.4	98,38
BARA TDJT BENZINARIE	0.4	98,91
Compartiment Benefic	20	100,15
Compartiment Benefic2	20	100,15
Compartiment ENEL	20	100,15
IS1	0.4	98,89
IS2.1	0.4	98,61
IS3.1	0.4	98,64
IS4.3	0.4	98,68
Post trafo 1 - 2000kVA	20	100,14
Post trafo 2 - 2000kVA	20	100,13
Post trafo 3 - 2000kVA	20	100,13
Post trafo 4- 2000kVA	20	100,12
Tablou SI	0.23	97,14

Based on the values presented in Tables 6.1–6.4, graphical representations were created to illustrate the variation of voltage drops, as well as the evolution of active and reactive power losses, under two distinct operating scenarios:

- the situation in which all charging stations are connected, and the 150 kWh storage systems installed at each transformer substation operate in discharging mode, supplying energy to the grid;
- the situation in which all charging stations are connected, and the 150 kWh storage systems installed at each transformer substation operate in charging mode, absorbing energy from the grid

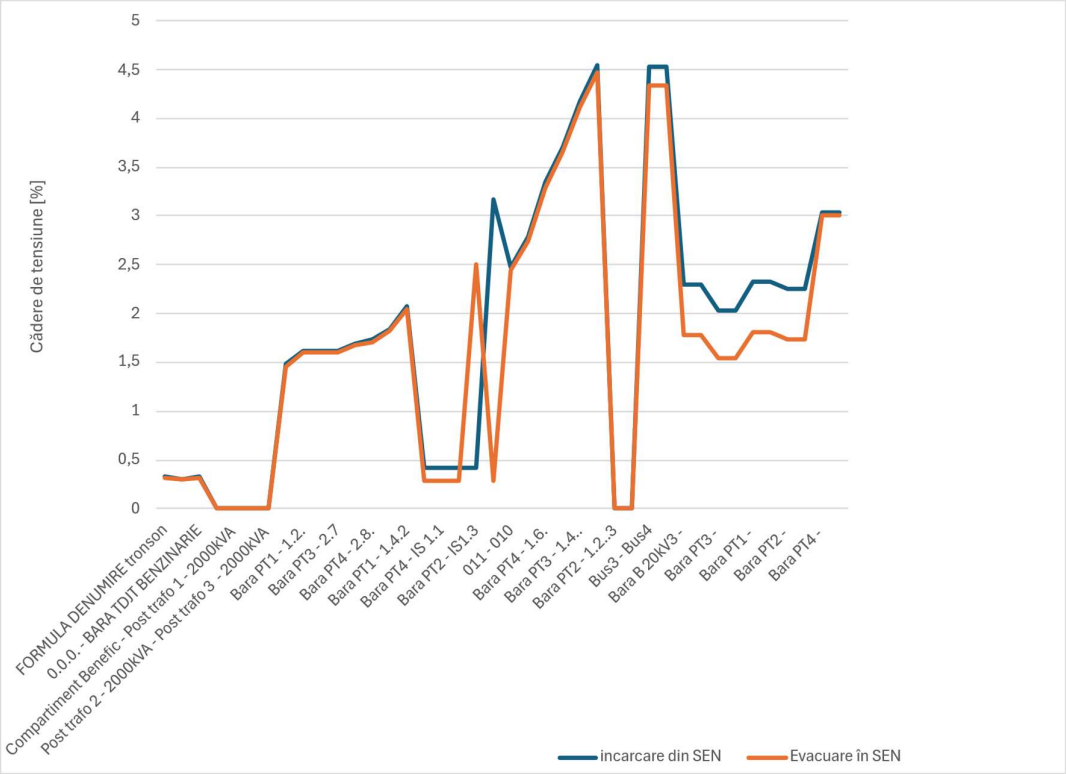


Fig. 6.13 Voltage drops for the two operating cases described above.

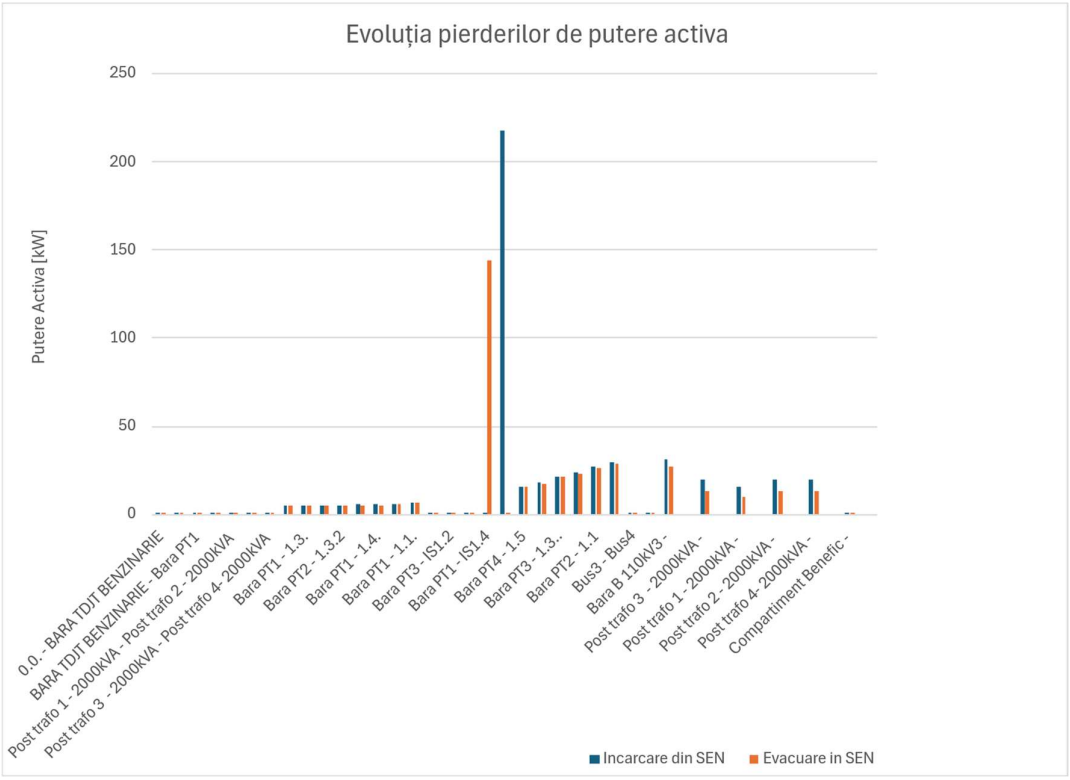


Fig. 6.14 Evolution of active power losses for the two operating cases described above.

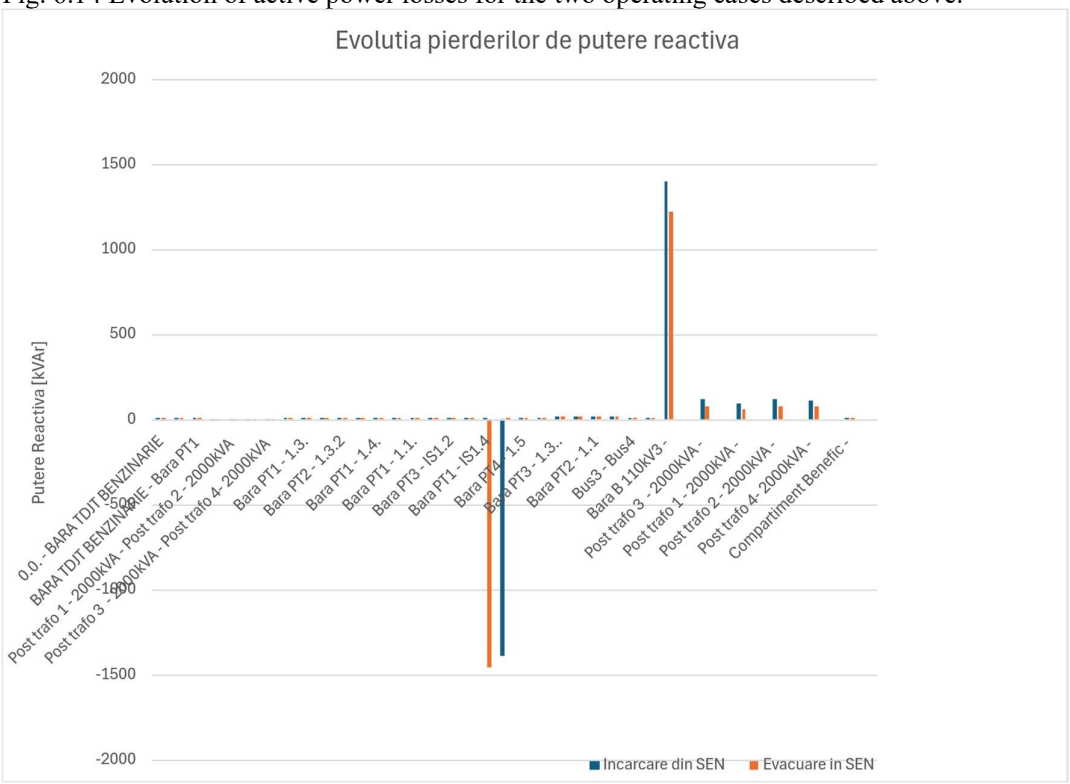


Fig. 6.15 Evolution of reactive power losses for the two operating cases described above.

7. CONCLUSIONS AND REMARKS

7.1 Conclusions

This doctoral thesis has approached, in an integrated manner, the analysis and modernization of electrical distribution systems in the context of the energy transition, digitalization, and the growing share of renewable sources. The research has demonstrated that smart grids, equipped with advanced automation and energy flow management functionalities, form the cornerstone of energy security and supply continuity for consumers.

The main conclusions can be summarized as follows:

- **Modernizing distribution infrastructure** through the implementation of remote control, automation, and SCADA systems leads to increased reliability, reduced losses, and improved performance indicators (SAIDI, SAIFI).
- **The integration of renewable sources and active users** brings sustainability and emission reduction benefits but introduces technical and operational challenges such as voltage regulation, protection selectivity, and reverse power flow phenomena.
- **The reverse power flow** has significant consequences on transformer operation, protection schemes, and the operational control regime of the network, requiring tailored solutions to ensure stability and operational safety.
- **Energy storage systems (BESS)** have been identified as key elements for network flexibility, demand–supply balancing, EV integration, and support of ancillary services.
- **The energy market analysis** highlighted the role of system services and capacity markets in maintaining energy balance and stimulating investments.
- **The case study regarding the design of a 6 MW charging station** validated the proposed concepts, demonstrating how electromobility infrastructure can be integrated into a modern, reliable distribution system.

The overall conclusion is that the transition toward intelligent and sustainable grids can only be achieved through a multidimensional approach combining technical, economic, and regulatory aspects. The obtained results form a solid foundation for future developments, such as the implementation of AI-based flexibility management algorithms, expansion of local energy markets, and strengthening grid resilience against climate and cyber risks.

Overall, the thesis contributes to establishing strategic directions in energy engineering, with a direct impact on increasing the efficiency, security, and sustainability of the national power system.

7.2 Personal Contributions

The author's doctoral research materialized through several scientific, technical, and applied contributions, derived from a complex research process involving theoretical, experimental, and documentary studies on modern power distribution systems. The research results were validated through publications in specialized journals and presentations at national and international scientific conferences, as follows:

Scientific Contributions (Published and Presented)

- Author of the article "Solutions for Increasing Efficiency in Distribution Networks", published in U.P.B. Scientific Bulletin, Series C, Vol. 87, Iss. 1/2025, ISSN 2286-3540.

- Paper presented and published in EMERG, Vol. XI, Issue 2/2025, pp. 111–131 (DOI: 10.37410/EMERG.2025.2.08), at the National Symposium on Power Quality, December 11–12, 2024, Târgoviște.
- Paper "New Solutions for Supplying High-Power Electric Vehicle Charging Stations", presented at New Technologies in Power Systems – CNR-CME & Siemens Energy Symposium, Sibiu, February 27–28, 2025.
- Author of the article "Effects of Reverse Power Flow", published in Mesagerul Energetic, Vol. XXV, No. 240, May–June 2025, pp. 14–17.
- Paper "Operational Management of the Power Distribution System in the Era of Digitalization and Artificial Intelligence", presented at SIREN – Romanian Energy Symposium, Bucharest, September 22–24, 2025, accepted for publication in EMERG, Vol. X, No. 3/2025.
- Co-author of "Electrical Protection of Microgrids", presented at SIREN – Romanian Energy Symposium, Bucharest, September 22–24, 2025, and accepted for publication in EMERG, Vol. X, No. 3/2025.

Technical Contributions

- Developed a comparative analysis of distribution network structures and operation, emphasizing the impact of automation and remote control on SAIDI and SAIFI indicators.
- Designed a methodology for assessing reverse power flow effects on transformer performance and network protection systems.
- Conducted an impact analysis of distributed generation and active users on distribution networks, focusing on protection, automatic voltage regulation, and islanded operation.

Applied Contributions

Developed an applied study for the design of a 6 MW fast-charging station integrated with photovoltaic generation and storage systems, validating the theoretical concepts proposed.

7.3 Future Research Directions

Relevant research directions derived from this thesis may include:

- **Implementation of artificial intelligence and machine learning algorithms for load forecasting**, fault diagnosis, and network reconfiguration optimization.
- **Development of advanced storage solutions** (hydrogen, supercapacitors, next-generation batteries) and their integration into unified operational frameworks with distribution networks.
- **Enhancement of network resilience** through cybersecurity strategies and improved response capacity to extreme events (storms, heatwaves, cyberattacks).
- **Integration of electromobility infrastructure** within a smart distribution system, capable of managing high power demand and providing ancillary services through the Vehicle-to-Grid (V2G) concept.